FISHERIES OCEANOGRAPHY

Fish. Oceanogr. 10 (Suppl. 1), 14–41, 2001

Ecological processes influencing mortality of juvenile pink salmon (*Oncorhynchus gorbuscha*) in Prince William Sound, Alaska

T. M. WILLETTE,[1] R. T. COONEY,[2]
V. PATRICK,[3] D. M. MASON,[4] G. L. THOMAS[5]
AND D. SCHEEL[5]

[1]*Alaska Department of Fish and Game, Division of Commercial Fisheries, 43961 Kalifornsky Beach Road, Ste B, Soldotna, AK 99669, USA*
[2]*306 10th Avenue NE, Choteau, MT 59422, USA*
[3]*University of Maryland, Office of Information Technology, Advanced Visualization Laboratory, College Park, MD 20742, USA*
[4]*NOAA Great Lakes Environmental Research Laboratory, 2205 Commonwealth Blvd., Ann Arbor, MI 48105, USA*
[5]*Prince William Science Center, PO Box 705, Cordova, AK 99574, USA*

ABSTRACT

Our collaborative work focused on understanding the system of mechanisms influencing the mortality of juvenile pink salmon (*Oncorhynchus gorbuscha*) in Prince William Sound, Alaska. Coordinated field studies, data analysis and numerical modelling projects were used to identify and explain the mechanisms and their roles in juvenile mortality. In particular, project studies addressed the identification of major fish and bird predators consuming juvenile salmon and the evaluation of three hypotheses linking these losses to (i) alternative prey for predators (prey-switching hypothesis); (ii) salmon foraging behaviour (refuge-dispersion hypothesis); and (iii) salmon size and growth (size-refuge hypothesis). Two facultative planktivorous fishes, Pacific herring (*Clupea pallasi*) and walleye pollock (*Theragra chalcogramma*), probably consumed the most juvenile pink salmon each year, although other gadids were also important. Our prey-switching hypothesis was supported by data indicating that herring and pollock switched to alternative nekton prey, including juvenile salmon, when the biomass of large copepods declined below about 0.2 g m⁻³. Model simulations were consistent with these findings, but simulations suggested that a June pteropod bloom also sheltered juvenile salmon from predation. Our refuge-dispersion hypothesis was supported by data indicating a five-fold increase in predation losses of juvenile salmon when salmon dispersed from near-shore habitats as the biomass of large copepods declined. Our size-refuge hypothesis was supported by data indicating that size- and growth-dependent vulnerabilities of salmon to predators were a function of predator and prey sizes and the timing of predation events. Our model simulations offered support for the efficacy of representing ecological processes affecting juvenile fishes as systems of coupled evolution equations representing both spatial distribution and physiological status. Simulations wherein model dimensionality was limited through construction of composite trophic groups reproduced the dominant patterns in salmon survival data. In our study, these composite trophic groups were six key zooplankton taxonomic groups, two categories of adult pelagic fishes, and from six to 12 groups for tagged hatchery-reared juvenile salmon. Model simulations also suggested the importance of salmon density and predator size as important factors modifying the predation process.

Key words: Pink salmon, juvenile, predation, numerical modelling, Salmon density, prey switching

INTRODUCTION

This component of the Sound Ecosystem Assessment (SEA) program focused on improving our understanding of the mechanisms influencing mortality of juvenile pink salmon (*Oncorhynchus gorbuscha*) in Prince William Sound (PWS), Alaska. Focus on this species resulted from very poor adult returns to PWS in 1992 and 1993 that devastated the commercial fishing industry dependent on them (Cooney *et al.*, 2001a; this volume p. 97). Charged by the fishing industry and other user groups in the region with developing a study plan to improve predictive capabilities, we first set out to properly bound the problem by identifying the lifestage of the target species (pink salmon) and the trophic processes to examine.

Poor returns of both wild and hatchery-reared stocks indicated that the run failures were caused by mortality during ocean lifestages, because hatchery stocks had been sheltered from natural mortality during earlier stages. We elected to focus on the early juvenile lifestage in part because mortality is typically very high during early sea life and may determine recruitment success in salmon (Parker, 1968; Ricker, 1976; Hartt, 1980; Bax,

Correspondence. e-mail: mark_willette@fishgame.state.ak.us

1983). Focus on this lifestage limited the temporal and spatial domain of our study to the initial 60 days of marine residence and to the waters within PWS.

Pink salmon exhibit a 2-year lifecycle, so adults returning each year reared in the sea as juveniles the previous year. Field studies examining the effects of the *Exxon Valdez* oil spill on juvenile pink salmon in the region had documented low juvenile growth rates in 1991 (Willette, 1996) and near average growth in 1992. An environmental monitoring program conducted by the Prince William Sound Aquaculture Corporation had also documented very low ocean temperatures in the spring of 1991, and near average ocean temperatures but a very weak zooplankton bloom during the spring of 1992. We recognized that slow-growing juvenile salmon could sustain higher mortality, because they are vulnerable to size-selective predators for a longer time (Parker, 1971; Healey, 1982; West and Larkin, 1987). While this process may have caused poor survival of juveniles in 1991, it could not have been the cause of the poor survival in 1992 because these fish exhibited near average growth rates as juveniles. These observations suggested that the weak zooplankton bloom in 1992 caused high mortality among juvenile salmon in some way other than depressed growth due to low prey densities.

Earlier research on juvenile pink salmon in PWS had examined many of the typical 'bottom-up' processes thought to affect mortality. As in other regions, juvenile pink salmon had been found to rear in nearshore habitats for several weeks after entering the sea (Cooney et al., 1981). Juveniles entering in bays quickly migrated to the many passages in the Sound (Wertheimer and Celewycz, 1996), where they initiated a general south-westward movement toward the Gulf of Alaska (Willette, 1996). During the first few days of sea life, harpacticoid copepods and calanoid copepods comprised about 70% and 10% of their diet (Cooney et al., 1981), but as the fish grew, large calanoid copepods comprised up to 90% of their diet (Sturdevant et al., 1996; Willette, 1996). Daily growth rates during this period ranged between 2 and 7% body weight per day, but growth was not always related to survival as would be expected if size-selective predation regulated mortality each year (Willette, 1996). Cooney et al. (1995) found that local stocks of wild pink salmon had evolved a timing mechanism allowing fry to enter PWS at exactly the time of a large calanoid copepod bloom each spring. This phenomenon initially appeared to be another example of the match-mismatch hypothesis in which the release of larvae is timed to match the production of their food (Cushing, 1967).

The match-mismatch hypothesis is based on the notion that recruitment success is driven by production from lower trophic levels (bottom up) through effects on larval growth. However, our observations in PWS led us to develop an alternative hypothesis to explain in part the remarkable correspondence between the migration of pink salmon into the sea and the timing of the annual copepod bloom. We conjectured that bottom-up effects on growth must be modified by interactions with animals at higher trophic levels (top down), because the larval and juvenile stages are very vulnerable to predation due to their small size (Sissenwine, 1984; Bailey and Houde, 1989; Sogard, 1997). This conjecture, which came to be known as the 'prey-switching hypothesis', focused our efforts on processes involving trophic levels immediately below and above our target species and involved macrozooplankton as alternative prey for animals that prey on juvenile salmon:

H_a: Annual losses of juvenile fishes to predation are determined by the numbers and kinds of predators and by the kinds and amounts of alternative prey, particularly macrozooplankton, available to these predators.

The spring bloom is an important period in the seasonal energy cycle for the later lifestages of many subarctic fishes (Paul et al., 1993; Smith and Paul, 1986). Movements of these larger animals into the surface layer to feed on macrozooplankton leads to an overlap in distribution of juvenile salmon with potential predators. The copepods *Pseudocalanus*, *Acartia*, and *Oithona* are numerically dominant in PWS during spring, but the much larger copepods *Neocalanus*, *Calanus*, and *Metridia* sometimes compose the majority of the biomass (Cooney et al., 2001b; this volume p. 1). *N. plumchrus* and *N. flemingeri* build a substantial high-energy lipid reserve which is utilized during the subsequent winter for egg development (Cooney, 1986). The relatively high-energy content of these copepods (Platt et al., 1969) makes them an attractive food source for many fishes. Large calanoid copepods compose a major part of the diets of herring and pollock during this season (Dwyer et al., 1987; Coyle and Paul, 1992; Yoshida, 1994), but both species are also piscivorous (Armstrong and Winslow, 1968; Thorsteinson, 1962; Bakshtansky, 1965; Dwyer et al., 1987). We conjectured that feeding mode shifts toward piscivory among these larger individuals may modify the mortality rates of larval or juvenile lifestages predicted by bottom-up processes.

Two additional major hypotheses emerged during the course of our 5-year study. The 'refuge-dispersion hypothesis' focused our efforts on juvenile salmon foraging behaviour and the overlap between distributions of predator and prey, while the 'size-refuge hypothesis' focused our efforts on processes affecting size-dependent predation losses of juvenile salmon. These two hypotheses are described and evaluated by Willette (2001; this volume p. 110).

Our approach to solving the problem posed by the fishing industry involved development of a mechanistic numerical foraging-physiology-dispersion model of the predator–prey interactions regulating juvenile salmon mortality (Patrick *et al.*, 2001). The model was used as a tool to integrate our knowledge of system function and examine processes that could not be directly observed. Field studies were directed at (i) identifying the predator taxonomic groups that accounted for the greatest predation losses of salmon; (ii) validating our numerical model; and (iii) testing our hypotheses related to mortality processes.

Our study was further bounded when we recognized the utility of using hatchery releases of tagged juvenile pink salmon as a tool for understanding mortality processes. In the mid-1970s, a salmon hatchery program was initiated in PWS. By the early 1990s, pink salmon were reared at four hatcheries and production exceeded 500 million fry (Fig. 1). Since 1988, about 1 million coded-wire tags (CWTs) were applied to the juvenile salmon released from PWS hatcheries (Geiger, 1990). Recoveries of these tagged fish as adults were used to estimate numbers of wild- and hatchery-origin salmon returning to PWS each year. Wild pink salmon spawn in about 1000 relatively short streams bordering PWS. Adult returns of wild pink salmon have fluctuated between 0.6 and 21.2 million since the early 1960s (Fig. 1b). The eastern and south-eastern districts of PWS probably account for over half of the approximately 185 million wild pink salmon fry that enter the sound from bordering streams (Fig. 1a). Fluctuations in total fry-to-adult survivals of hatchery pink salmon and return per alevin for wild salmon have been generally coherent suggesting that similar processes have affected survival of both groups (Fig. 1c).

The hatchery program in PWS applied unique tag codes to up to 12 groups of juvenile salmon released from each hatchery each year. The rich structure in these CWT data proved to be critical to furthering our understanding of the ecological processes affecting juvenile salmon mortality. Although the total survival of pink salmon returning to PWS hatcheries generally fluctuated by a factor of 3 (Fig. 1), the survivals of individual CWT groups released from various hatcheries fluctuated by an order of magnitude (Willette *et al.*, 1999b). Each of the individual CWT groups released from the hatcheries experienced a different time evolution of the zooplankton bloom because the various groups were released on different dates during the bloom and at various locations in PWS. The mean size of the individuals in each group also varied by nearly an order of magnitude, and the numbers of individuals released in each group varied by a factor of 4. Our use of tagged hatchery salmon as a tool

further focused the spatial domain of our study to the western perimeter of PWS because this was a known migration corridor for hatchery-reared juvenile pink salmon (Willette, 1996).

In this paper, we first present an analysis of field data intended to provide order-of-magnitude estimates of predation losses of salmon to various predator taxonomic groups. This analysis was conducted only to identify those groups that could be neglected in the numerical model and thus further bound the problem. We then present validation analyses of our numerical model by comparing model simulations with field estimates of juvenile salmon growth, diet, and survival, as well as predator diet and prey size distributions. We then use our model to examine ecological processes affecting juvenile salmon mortality that were not directly observed. Finally, we evaluate our three major hypotheses, synthesizing our findings from field and modelling studies.

METHODS

Field sampling

Our field sampling focused on describing the time evolution of the predator–prey interactions affecting juvenile salmon released from the Wally H. Noerenberg Hatchery (WHN) in north-western PWS (Fig. 1a). We took this approach because the migration of fish released from this hatchery was bounded by the passages in western PWS (Willette, 1996). In 1994, we sampled the migration of CWT juvenile salmon released from WHN Hatchery and juvenile salmon predators and prey along the salmon migratory pathway (Willette *et al.*, 1995a, 1995b). Analyses of dietary overlap among various juvenile fishes including juvenile salmon were also conducted in 1994 (Willette *et al.*, 1997).

After 1994, our sampling program was designed to sample multiple sites each year (Fig. 1a) exhibiting a range of zooplankton biomass and juvenile salmon relative abundances. A stratified-systematic sampling design was used to sample the following parameters at each site: (i) juvenile salmon relative abundance; (ii) juvenile salmon diet composition; (iii) juvenile salmon size composition; (iv) predator relative abundance; (v) predator species and size composition; (vi) predator diet composition; and (vii) surface-layer macrozooplankton density and composition. Sampling was stratified between nearshore and offshore habitats and by time of day (3-h periods). The 20-m isobath was chosen as the boundary between nearshore and offshore habitats, because kelp beds typically extended to this water depth. Willette (2001; this volume p. 110) describes these sampling methods in greater detail.

Figure 1. (a) Locations of pink salmon hatcheries (bold type) and salmon management districts (solid lines) in Prince William Sound and estimated mean annual numbers of wild and hatchery juvenile salmon entering each district. Dashed lines indicate area of juvenile salmon migratory pathway sampled during SEA pink salmon studies in 1994, and solid circles indicate sites sampled in 1995–97, (b) historical time series of adult returns of wild and hatchery pink salmon to Prince William Sound, and (c) historical time series of wild salmon adult returns per alevin index (number m^{-2}) and hatchery salmon survivals.
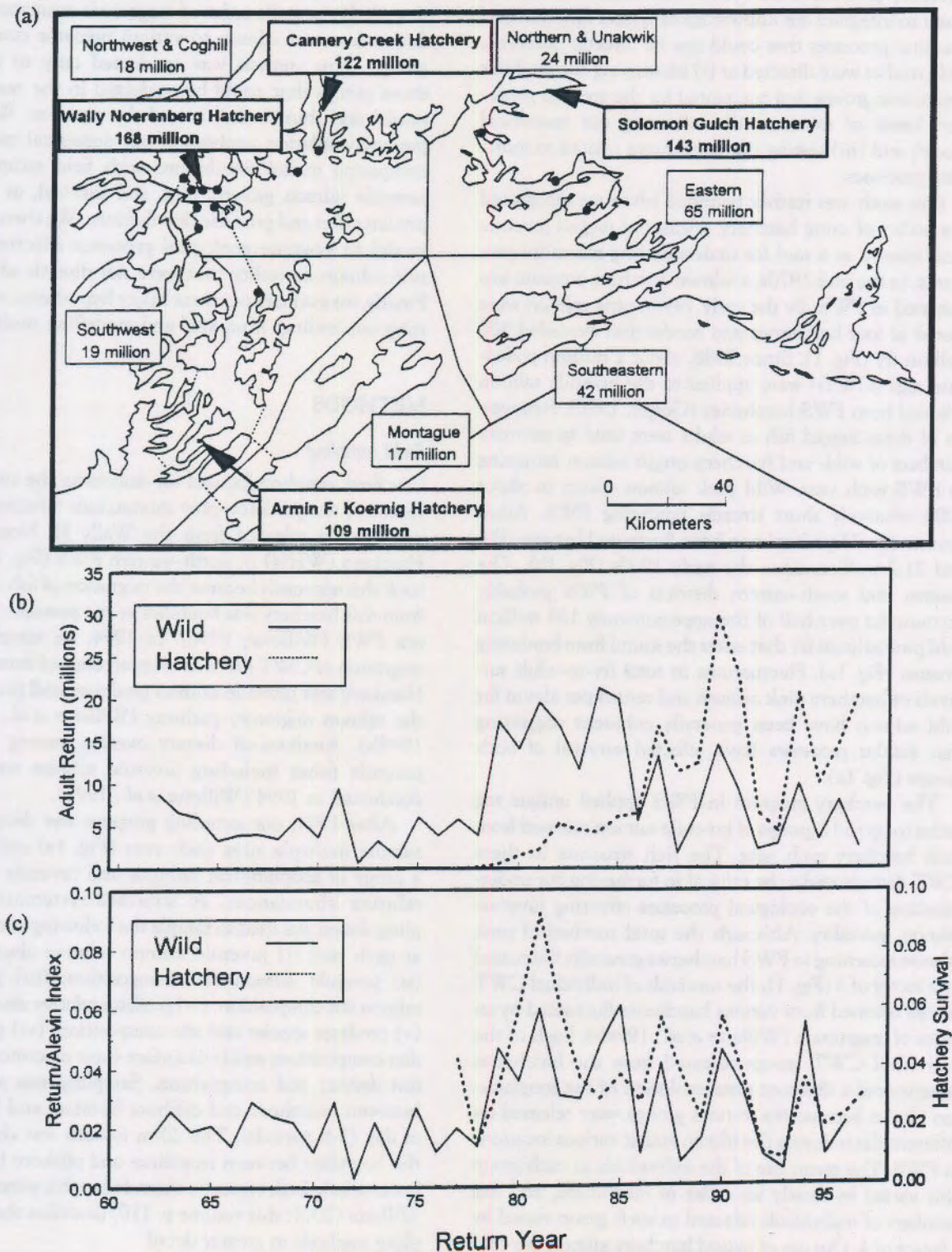
In 1995, the diel foraging behaviour of juvenile salmon and their predators was examined at 16 sites adjacent to WHN Hatchery, and samples of juvenile salmon were collected for analysis of whole body energy content (Paul and Willette, 1997). In 1995, field counts of seabirds and observations of feeding rates for plunge-diving seabirds were also obtained during salmon fry releases from WHN Hatchery between April and June. The mortality of salmon due to seabird predation was estimated from these field observations and energetic models (Scheel and Hough, 1997).

In 1996 and 1997, sampling was conducted over the 12-h period spanning the night at about 24 sites each year, and differences in size and condition between wild- and hatchery-origin juveniles were examined using otolith thermal marks to identify each group. Sampling was restricted to the 12-h period spanning the night because our observations in 1995 indicated that predation on juvenile salmon was probably greater during that time. Restricting the duration of sampling at each site also allowed us to expand the spatial coverage of our sampling effort. In 1996, several sites near Cannery Creek Hatchery were sampled and, in 1997, four sites in eastern PWS were sampled.

A variety of gear types were used to sample juvenile salmon and their predators in nearshore and offshore habitats at each site. During 1994–96, a mid-water wing trawl (40×28 m) was used to sample potential predators in the 0–60 m layer of the water column, and the trawl vessel collected at least two zooplankton samples each day using a 0.5-m diameter ring net (335-μm mesh) towed vertically from a depth of 50 m at mid-passage stations. During all 4 years of the study, purse seines were used to sample predators and juvenile salmon in off-shore habitats, and a small-mesh purse seine deployed from a skiff sampled juvenile salmon inshore of the 20-m isobath. Beginning in 1995, potential predators were sampled with variable-mesh gill nets set out from shore at two stations. In each study area, temperature and salinity were measured with a conductivity-temperature-depth profiler (CTD) to a depth of 100 m. A pyro-meter equipped with a quantum sensor was used to measure ambient light intensity at 30-min intervals. A total of 423 trawl sets, 1069 purse seine sets, and 2664 gill net sets were made during the 4 years of the study. Willette *et al.* (1999a) and Willette (2001; this volume p. 110) provide more detailed descriptions of field sampling methods, and descriptions of labor-atory methods used to analyse zooplankton and stomach samples.

Acoustic techniques for echointegration and dual beam processing of target strength were used to estimate the biomass of potential predators on salmon in pelagic habitats (MacLennan and Simmonds, 1992; Thomas *et al.*, 1997). Acoustic surveys were conducted using sphere-calibrated BioSonics 101 (120 and 200 kHz) and 102 (38 kHz) dual beam echosounders with BioSonics ESP/EI and DB software programs. Each sonar system was equipped with a GPS receiver to geo-reference acoustic data. Measured target strengths of individual fish were compared with length data of fish captured with nets. To establish a fish size-target strength relationship, we used the relationships of Thorne (1983) for target strength per kg vs. length, Traynor and Ehrenberg (1979) for wall-eye pollock target strength vs. length, and MacLennan and Simmonds (1992) for Pacific herring target strength vs. length. A stratified-systematic design was used for acoustic surveys with a series of evenly spaced parallel transects orthogonal to the coastline. Long day-lengths necessitated daylight surveys to monitor predator densities in the spring. When surveys were conducted at night, only red running lights were illuminated. Weighted mean densities and their variances were com-puted and extrapolated to biomass and 95% confidence limits calculated.

Identification of important predators

Total consumption of juvenile salmon was estimated for nine taxonomic groups of fish predators during three sampling periods (early May, late May, and early June) using field data from 1995 to 1997. The nine pred-ator groups were herring (*Clupea pallasi*), immature (age 1–2) and adult (age 3+) walleye pollock (*Theragra chalcogramma*), other gadids (*Gadus macrocephalus, Microgadus proximus*), adult salmon (*Oncorhynchus* spp.), trout (*Salvelinus malma, O. mykiss*), benthic fishes (Cottidae, Hexagrammidae, Stichaeidae, Cyclopteridae, Zoarcidae, Bathymasteridae), pelagic rockfishes (*Sebastes melanops, S. ciliatus, S. flavidus*) and demersal rockfishes (*Sebastes nebulosus, S. caurinus, S. maliger, S. rubberimus,* and others). Data collected in 1994 were not included in the analysis, because we did not adequately sample other gadids, benthic fishes, and rockfishes that year. Total consumption (C) of juvenile salmon by predator group *i* was estimated from

$$C_i = I_i D_i A_i T, \tag{1}$$

where I_i was the mean daily individual predator con-sumption of juvenile salmon (number of salmon con-sumed day^{-1}) for group *i* (Willette, 2001; this volume p. 110; Table 9), D_i was the predator density (number of predators m^{-2}) of group *i*, A_i was the area (m^2) occupied by group *i*, and *T* was the number of days during each period. Willette (2001; this volume) described the methods used to estimate the mean daily individual predator consumption of salmon by each group.

The width of the nearshore zone in which the predator–prey interaction occurred and the density of predators within this zone were important in evaluating total predation losses. We used our knowledge of the total abundance and distribution of these fishes in PWS to derive order of magnitude estimates of these parameters, but we recognized that temporal and spatial variation was considerable. For herring, we assumed that a biomass of 29 000 metric tons (mt) (Morstad et al., 1997) was distributed in a 1.0-km wide band along the 1800-km length of shoreline in PWS (excluding small bays). For adult pollock, we used our mean acoustic density estimate from 1994 to 1997 (2.5×10^{-3} m^{-2}) and assumed that pollock were distributed throughout PWS (Haynes et al., 1995; Thomas et al., 1998). This resulted in a total pollock biomass of 18 700 mt, which was about one half of the pollock biomass that spawned in south-west PWS in the winter of 1997 (Kirsch, pers. comm.). For salmon, we assumed a population size of 3 million based upon reconstructed run sizes during May–June (Morstad et al., 1997). For trout (primarily Salvelinus malma), we assumed a population size of 156 000 based upon available overwintering habitat for this species in lakes bordering PWS (Hepler et al., 1994). We assumed salmon and trout were distributed within a 1.0-km wide band along the shoreline, because these species were commonly captured in purse seines fished within this zone and very few were captured in trawls further offshore. For all other predators, a 0.1-km wide band was assumed, because this was the approximate width of the nearshore zone shallower than 20-m depth, and many of the other predator species were associated with kelp that only occurred in this zone. Density estimates provided by Paulsson (pers. comm.) were used for rockfishes, Jewett and Dean (1997) for other gadids and age 1–2 pollock, and Jewett et al. (1995) for benthic fishes. Abundances of immature pollock were assumed to increase by a factor of 2, and salmon and trout by a factor of 10 from early May to June based upon catch per net set in variable-mesh gillnets and purse seines (Willette, 2001; this volume p. 110; Table 6). Abundances of adult pollock were assumed to decrease by a factor of 0.5 during this same period based upon catch per hour in mid-water trawls (Willette, 2001; this volume; Table 6). No seasonal changes in abundance were assumed for the other groups. The probable range of predator consumption of salmon was calculated by multiplying the point estimate of predator abundance by the observed percent deviation of mean catch per net set among years (1995–97) for each predator group (Willette, 2001; this volume; Table 7). Finally, estimates of total consumption of salmon were calculated for three predator functional groups (facultative planktivores, piscivores, and invertebrate feeders) based upon their diets (Willette, 2001; this volume).

Simulation of predator–prey interactions: model structure

We developed a numerical foraging-physiology-dispersion model of the predator–prey interactions affecting mortality of juvenile salmon in PWS (Patrick et al., 2001). The model was designed around an abstraction of the actual system derived from our collective knowledge of the key system elements and functions, as well as the data structures available for model inputs or for model calibration and validation. Each of the four hatcheries in PWS released from six to 12 CWT groups at various times during the spring bloom period, 1994–95. Our ability to track the survival and spatial distribution of these fish released at different times, and at various densities, sizes, and locations in PWS provided a rich data structure for model validation. Our conceptual model reduced the trophic structure of the natural system to two planktivore predators differentiated mainly by size, six taxonomic groups of zooplankton, and several CWT groups of salmon (Fig. 2). In our conceptual model, zooplankton was prey for pollock, herring and juvenile salmon, whereas juvenile salmon were also potential prey for pollock and herring. The foraging and bioenergetics of the planktivore predators and each CWT group of salmon was modelled with the mass flux between groups modulated primarily by temperature,

Figure 2. Conceptual model of juvenile pink salmon ecology in Prince William Sound. CWT indicates coded-wire tag groups released from each hatchery. Arrows indicate mass flux among trophic groups modulated by light intensity, temperature, prey density, and prey size.
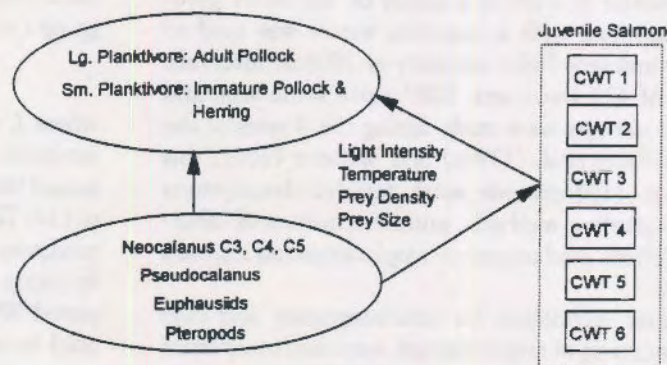
light intensity, and the density and size of zooplankton as forcing variables (Fig. 2).

The foraging and physiology of juvenile salmon and their predators were modelled using integrated foraging, gastric evacuation, and physiology submodels (Patrick *et al.*, 2001). Foraging rate (v_f^q, number of trophic group f consumed by trophic group q per unit time) was modelled using a modified Holling type II model (Holling, 1959) with handling time partitioned into the time required to attack prey, capture prey and a satiation or wait time, i.e.

$$V_f^q = \frac{u_f \hat{\epsilon}_f^q s_f \alpha_f'^q C_f^q}{1 + \sum_{f=1}^{N} u_f \hat{\epsilon}_f^q s_f \alpha_f'^q (h_{Af}^q + C_f^q h_{Cf}^q + m_f C_f^q \zeta_q)} \quad (2)$$

where u_f was the density of group f, $\hat{\epsilon}_f^q$ was the encounter rate of group q with group f (for a unit density of targets), S_f was a schooling factor that reduced the encounter rate to adjust for targets that present themselves as target clusters, $\alpha_f'^q$ was the probability of attack by an individual of group q upon an individual or cluster of individuals of group f given that a detection had occurred (this notation denotes the specific choice among all possible preys that maximized the mass flux of prey consumed), C_f^q was the probability that an individual of group q captured and ingested an individual of group f given that an attack had occurred, h_{Af}^q was the handling time associated with an attack by an individual of group q on an individual of group f, h_{Cf}^q was the handling time associated with the capture and ingestion of an individual of group f by an individual of group q, ζ_q was a satiation feedback wait time given an individual of group q had captured an individual of group f with mass m_f, and N was the number of f groups (Patrick *et al.*, 2001). Gastric evacuation rates were modelled as a function of temperature for both juvenile salmon (Brett and Higgs, 1970) and their predators (Smith *et al.*, 1989). The bioenergetics submodel simulated respiration rate,

a metabolic buffer representing blood glycogen, and growth rate of juvenile salmon and their predators. Respiration rates were modelled as combined standard, active, and feeding metabolic rates. Standard metabolism was a function of temperature, active metabolism was a function of swimming speed that varied with temperature, and feeding metabolism was a function of foraging rate (Patrick *et al.*, 2001).

An early priority for the foraging-physiology submodel was representation of the presumed ability of facultative planktivores to use both particle and ram filter-feeding modes (Willette *et al.*, 1999a). The parameters defined above for Equation 2 are for particle-mode foraging, the mode used by juvenile fish and piscivores. The model for ram foraging is obtained by redefining four parameters in Equation 2: (i) the encounter rate is redefined by replacing the reaction distance (i.e. distance for prey detection) by an effective radius of the mouth gape during ram feeding; (ii) attack probabilities and schooling factors are redefined to unity; (iii) capture probabilities for fish are set to zero and for zooplankton are set to either zero or unity according to an observed minimum ingested size or filtering threshold; and (iv) handling time is neglected. A facultative planktivore forager is assumed to be continuously comparing the potential mass intake for each of the two foraging modes and applying the mode providing the maximum foraging rate (Patrick *et al.*, 2001).

The structure of our foraging-physiology submodel was unique, because the submodels were integrated by a satiation function and a feedback loop that reduced foraging intake as satiation increased and drew down energy stores to fuel elevated activity during foraging (Fig. 3). Satiation was a function of gut fullness and available short-term energy reserves (blood glycogen levels). When the fish was actively feeding and the buffer was not full, 90% of the mass flux went into the buffer. As the gut or buffer filled, a satiation function reduced the foraging rate and the feeding metabolic demand on
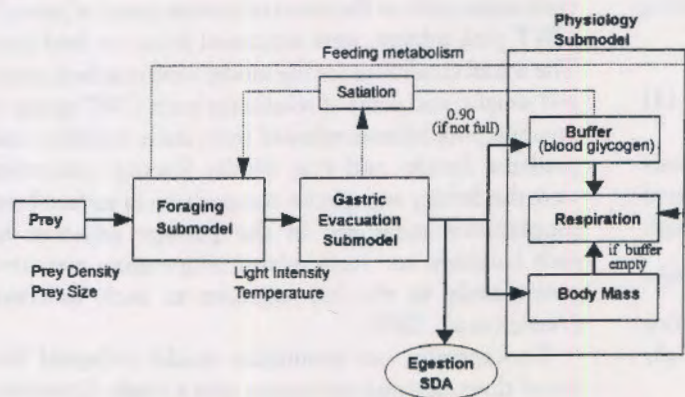

Figure 3. Structure of our foraging-physiology submodel. A feedback loop drew down energy stores to fuel elevated activity during foraging (dashed line). When the fish was actively feeding and the buffer was not full, 90% of the mass flux went into the buffer. As the buffer filled, a satiation function reduced the foraging rate (dashed line) and the feeding metabolic demand on the buffer. Satiation was a function of gut fullness and available short-term energy reserves (blood glycogen levels).

Figure 4. Left panel: One-dimensional migratory pathway used to model migration of juvenile salmon in western Prince William Sound. Values in circles indicate the number of kilometres from the Gulf of Alaska. Right panel: Schematic indicating the migration of multiple CWT groups of juvenile pink salmon along the one-dimensional migratory pathway at day of the year 120 and 145. The dispersion-taxis submodel simulated the migration and dispersion of salmon along the migratory pathway.
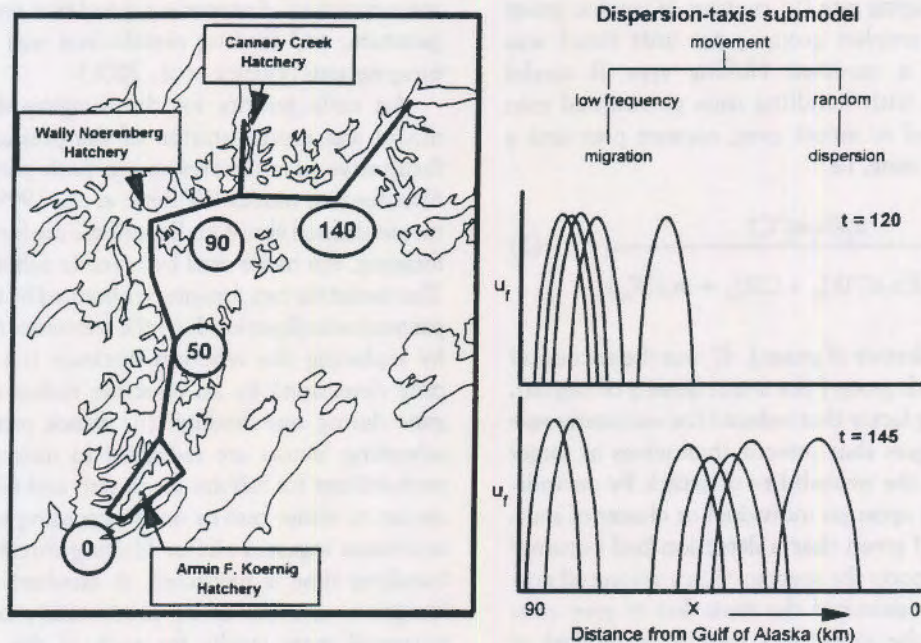
the buffer. This model structure enabled simulation of continuous feeding of juvenile salmon (Godin, 1981) and episodic feeding observed at times in adult fish (Helfman, 1993).

A dispersion-taxis submodel simulated the movement of each CWT group of juvenile salmon along a one-dimensional pathway from hatchery release sites to the Gulf of Alaska (Fig. 4). The dispersive component of the movement was represented as a basic Fickian diffusion with a constant diffusion coefficient (Ito, 1992). The taxis component of the movement was represented by an advection velocity tangent to the migration path and of constant speed. The submodel simulated the time varying density ($u_f(x, t)$) of each group of salmon along their migratory pathway, i.e.

$$\frac{\partial u_f}{\partial t} = D_f \cdot \frac{\partial^2 u_f}{\partial x^2} + \frac{\partial}{\partial x} u_f |v_{migr,f}| - \sum_q u_q v_f^q, \qquad (3)$$

where D_f was a diffusion coefficient, $|v_{migr,f}|$ was a constant migration speed set equal to the mean speed exhibited by juvenile CWT pink salmon migrating though PWS, and $-\sum_q u_q v_f^q$ was the number flux of juvenile salmon consumed by predators along the migratory pathway which modified salmon density (Patrick *et al.*, 2001).

The evolution of juvenile CWT salmon populations along the migratory pathway was modelled by simultaneously solving a series of ordinary or partial differential equations (Patrick *et al.*, 2001) for the food consumption (a_f), metabolic buffer (b_f), mass (m_f), length (l_f), and density (u_f) of each CWT group of salmon and the food consumption (a_q), metabolic buffer (b_q), mass (m_q), and length (l_q) of their planktivore predators along this one-dimensional migratory pathway (Fig. 5). The dispersion-taxis submodel was coupled with the foraging-physiology submodel through the number flux of salmon consumed by predators. Most model parameters were obtained from the literature, except system specific parameters, such as the mean migration speed of juvenile CWT pink salmon, were estimated from our field data. The initial conditions for the model were numbers, mean wet weight, and dates of release for each CWT group of juvenile pink salmon released from each hatchery, and predator density and size. Model forcing conditions were the density and species composition of surface layer zooplankton measured in the passage adjacent to each hatchery, and surface-layer temperature measured continuously in the bay adjacent to each hatchery (Patrick *et al.*, 2001).

Conceptually, our simulation model collapsed the actual three-dimensional system into a single dimension

Figure 5. Internal structure of our foraging-physiology-dispersion model. The time evolution of the development of CWT salmon populations was modelled by simultaneously solving a series of ordinary or partial differential equations for the food consumption (a_f), metabolic buffer (b_f), mass (m_f), length (l_f) and density (u_f) of each CWT group of salmon, and the food consumption (a_q), metabolic buffer (b_q), mass (m_q), and length (l_q) of their planktivore predators along a one-dimensional migratory pathway composed of x elements. The dispersion-taxis submodel simulated the movement of juvenile salmon along the migratory pathway. It was coupled with the foraging-physiology submodel through the number flux ($\sum_f u_q v_f^q$) of each CWT group of salmon consumed by planktivore predators which modified salmon density. The mass flux among trophic groups (heavy solid lines) is indicated by $\sum \gamma_f^q$. Population sizes are indicated for each CWT group of salmon at their release ($N_{f_i(t=0)}$), at their emigration from PWS ($N_{f_i(t=juv)}$), and when they return as adults ($N_{f_i(t=ret)}$). Model performance was evaluated by comparing mass, length, food consumption, and diet of juvenile salmon and their planktivore predators, as well as, patterns of survival (S_{ret_i} vs. S_{juv_i}) among multiple CWT groups by their date of release (dashed lines).
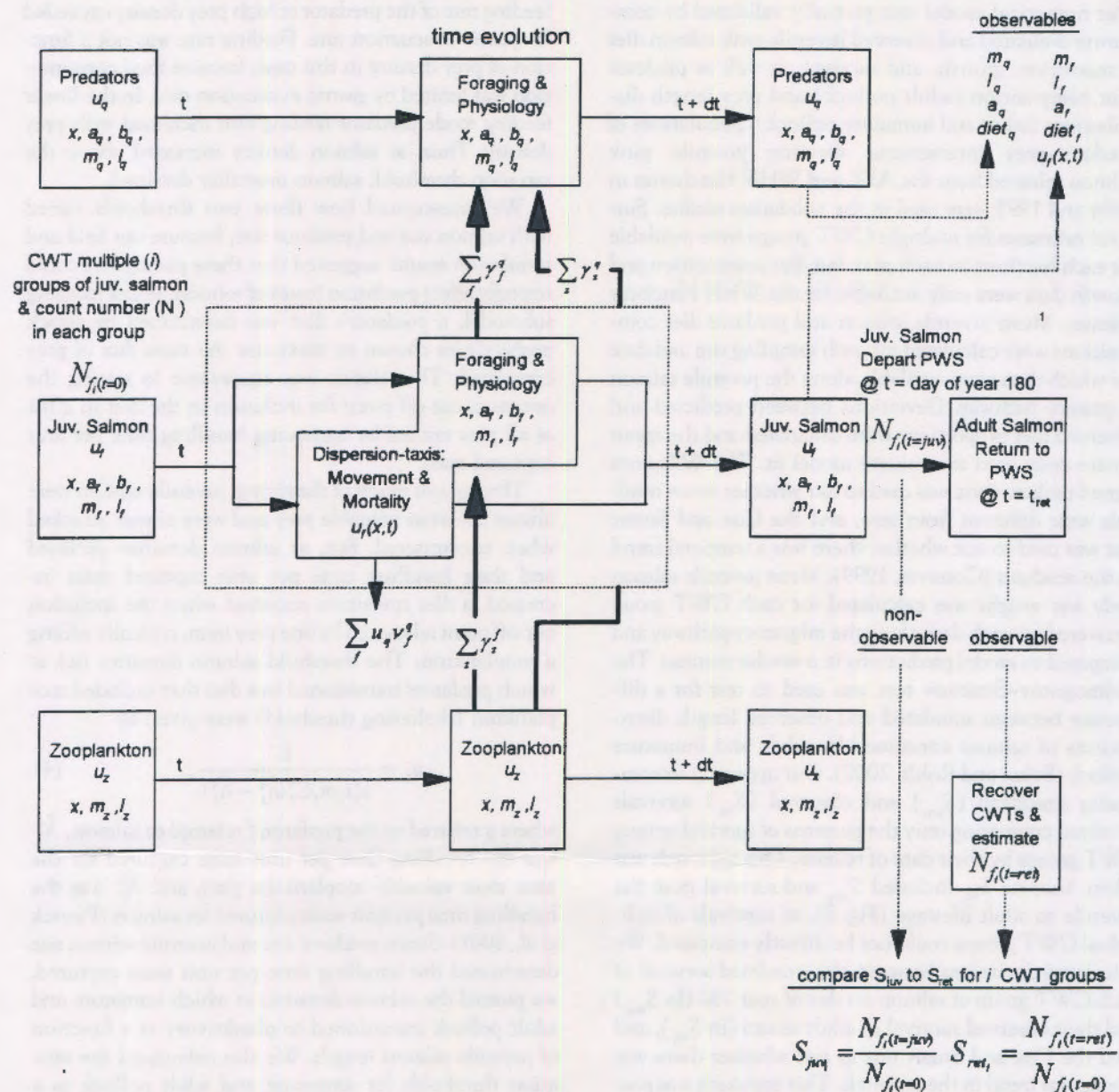
in which all predators present at a specific location encountered salmon as they migrated from the hatcheries. This characteristic of the model differed from the actual system, because only a small fraction of the predators present in our survey area actually encountered salmon. This model structure resulted in higher simulated predator consumption of salmon than we observed at any specific place and time in PWS because we could not instantaneously sample all predators encountering salmon in the actual system.

Simulation of predator–prey interactions: model validation

Our numerical model was partially validated by comparing simulated and observed juvenile pink salmon diet composition, growth, and survival, as well as predator diet composition (adult pollock) and prey length distributions (adult and immature pollock). Simulations of predator–prey interactions affecting juvenile pink salmon released from the AFK and WHN Hatcheries in 1994 and 1995 were used in the validation studies. Survival estimates for multiple CWT groups were available for each hatchery in each year, but diet composition and growth data were only available for the WHN Hatchery releases. Mean juvenile salmon and predator diet compositions were calculated for each sampling site and date for which data were available along the juvenile salmon migratory pathway. Deviations between predicted and observed diet proportions were calculated and the mean square error used to evaluate model fit. The Wilcoxon signed rank statistic was used to test whether mean residuals were different from zero, and the Cox and Stuart test was used to test whether there was a temporal trend in the residuals (Conover, 1999). Mean juvenile salmon body wet weight was calculated for each CWT group recovered on each date along the migratory pathway and compared to model predictions in a similar manner. The Kolmogorov–Smirnov test was used to test for a difference between simulated and observed length distributions of salmon consumed by adult and immature pollock (Sokal and Rohlf, 2000). Our approach to comparing simulated (S_{juv_i}) and observed (S_{ret_i}) survivals involved comparing only the patterns of survival among CWT groups by their date of release. This approach was taken, because S_{ret_i} included S_{juv_i} and survival from the juvenile to adult lifestage (Fig. 5), so survivals of individual CWT groups could not be directly compared. We calculated deviations between the simulated survival of each CWT group of salmon on day of year 180 (ln S_{juv_i}) and their observed survival to adult return (ln S_{ret_i}), and used the Cox and Stuart test to test whether there was a temporal trend in the residuals. This approach was possible, because multiple CWT groups had been released from each hatchery each year.

Simulation of predator–prey interactions: analysis of ecological processes

The structure of our numerical model suggested two threshold salmon densities separating three zones in which the relationship between salmon density and mortality differed. A 'sheltering threshold' was associated with a transition from predators feeding exclusively on juvenile salmon to inclusion of alternative zooplankton prey in their diet. A 'satiation threshold' involved a transition from predator satiation to a linear feeding mode. Predator satiation occurred when the potential feeding rate of the predator at high prey density exceeded its gastric evacuation rate. Feeding rate was not a function of prey density in this case, because food consumption was limited by gastric evacuation rate. In the linear feeding mode predator feeding rate increased with prey density. Thus, as salmon density increased above the satiation threshold, salmon mortality declined.

We investigated how these two thresholds varied with salmon size and predator size, because our field and simulation results suggested that these parameters could strongly affect predation losses of salmon. In our foraging submodel, a predator's diet was determined by attack probabilities chosen to maximize the mass flux of prey consumed. This choice was equivalent to setting the optimum cut-off point for inclusion in the diet in a list of all prey ranked by increasing handling time per unit captured mass.

Throughout much of the spring, juvenile salmon were always the most valuable prey and were always attacked when encountered. But, as salmon densities declined and their handling time per unit captured mass increased, a diet transition occurred when the inclusion cut-off point advanced by one prey item, typically adding a zooplankton. The threshold salmon densities (u_f) at which predators transitioned to a diet that included zooplankton (sheltering threshold) were given by

$$u_f = \frac{1}{\hat{e}_f^q s_f m_f C_f^q (\hat{h}_z^q - \hat{h}_f^q)}, \qquad (4)$$

where q referred to the predator, f referred to salmon, $\hat{h}_z^q$ was the handling time per unit mass captured for the next most valuable zooplankton prey, and $\hat{h}_f^q$ was the handling time per unit mass captured for salmon (Patrick et al., 2001). Since, predator size and juvenile salmon size determined the handling time per unit mass captured, we plotted the salmon densities at which immature and adult pollock transitioned to planktivory as a function of juvenile salmon length. We also calculated the satiation thresholds for immature and adult pollock as a function of salmon length. Predator feeding rates were calculated using Equation 2 and converted to mass using

a length-weight regression for salmon in PWS. Gastric evacuation rates of pollock at 6 °C were estimated using functions provided by Smith *et al.* (1989).

The proportional change in the number of salmon consumed before and after the transition to planktivory $\left(\dfrac{v_f^q}{v_f'^q} \right)$ was given by

$$\frac{v_f^q}{v_f'^q} = \frac{1}{1 + (u_z \hat{\varepsilon}_z^q h_z^q)(1 - \hat{h}_f^q / \hat{h}_z^q)}, \qquad (5)$$

where v_f^q was the number flux of prey f to predator group q after the transition to planktivory, $v_f'^q$ was the number flux of prey f to predator group q before the transition to planktivory, u_z was the density of the next most valuable zooplankton prey, $\hat{\varepsilon}_z^q$ was the predator's unit density encounter rate with that prey, and h_z^q was the handling time associated with the attack and capture of zooplankton prey (Patrick *et al.*, 2001). We examined the degree of sheltering by zooplankton in relation to predator

and salmon size by plotting $\dfrac{v_f^q}{v_f'^q}$ as a function of zooplank-

ton density and juvenile salmon size for immature and adult pollock as predators and *Neocalanus* stage 4, *Neocalanus* stage 5, and pteropods as alternative zooplankton prey.

Finally, we examined the effects of predator and prey densities, sizes, and growth rates on salmon survival when salmon densities were above the satiation threshold. When predators were satiated, salmon survival on day t after release (S_t) was given by

$$S_t = \frac{u_f(t)}{u_f(0)} = 1 - K_f^q (1 - e^{-(g_f - g_q)h}), \qquad (6)$$

where u_f was juvenile salmon density, and g_f and g_q were the growth rates of juvenile salmon and their predators (Patrick *et al.*, 2001). The constant (K_f^q) was given by

$$K_f^q = \frac{u_q m_q(0)}{u_f m_f(0)} \cdot \frac{\rho_q}{g_f - g_q}, \qquad (7)$$

where u_q was the density of the predator, m_q was the initial mass of the predator, u_f was the initial density of juvenile salmon, m_f was the initial body mass of juvenile salmon, and ρ_q was the maximum daily ration of the predator (Patrick *et al.*, 2001). Salmon populations crashed or bloomed according to whether K_f^q was greater or less than 1. We used this solution to simulate population trajectories for salmon released at high densities (sufficient to satiate predators) given observed densities of pollock in PWS (Table 1), maximum pollock growth rates (Smith *et al.*, 1986), and the range of salmon growth rates observed in PWS (Willette, 1996). Equations 4–7

were derived through qualitative analyses of our numerical model, see Patrick *et al.* (2001) for more detail.

RESULTS

Identification of important predators

We estimated that 534 million juvenile salmon were consumed by nine taxonomic groups of fish predators from early May to mid June (Table 1), and 8–17 million salmon were consumed by various seabirds (Scheel and Hough, 1997). Facultative planktivores probably consumed the greatest numbers of juvenile salmon (289 million: range 92–529), but piscivores also consumed significant numbers of salmon (232 million: range 135–370). The importance of each group probably varies considerably among years due to changes in spatial overlap between predator and prey, individual predator consumption rates, and predator year-class dominance. The high predation losses attributed to herring and pollock resulted from their much greater abundance compared to the other taxonomic groups, even though individual daily consumption of salmon by them was quite low (Willette, 2001; this volume p. 110). Avian predators exhibited much higher individual daily consumption of salmon than fish predators. In 1995, black-legged kittiwakes consumed 225–550 salmon day⁻¹, Bonaparte's gulls 150–300 day⁻¹, and Arctic terns 150–200 day⁻¹ (Scheel and Hough, 1997). Among fish predators, the numbers of juvenile salmon consumed each day were generally low and highly variable (Willette, 2001; this volume p. 110). However, Scheel and Hough's (1997) estimates were based upon observations of birds feeding on schools of juvenile salmon or upon energetic models that assumed that juvenile salmon were the only prey. Willette's estimates (this volume) were based upon stomach content analyses of fish collected at several sites where juvenile salmon were present at various densities. Other preys (zooplankton, benthic invertebrates, etc.) often dominated the diets of these fish (Willette, 2001; this volume).

Abundances of seabirds feeding on juvenile salmon declined from early May to June, whereas the relative abundance of three taxonomic groups of potential fish predators on salmon increased during this period. In 1995, counts of piscivorous seabirds near the WHN Hatchery declined from about 400 in early May to less than 100 in early June (Scheel and Hough, 1997). This seasonal decline in seabird abundance was attributed to either a decline in the density of juvenile salmon available to the birds or availability of other prey sources such as herring or sandlance. Catch per hour of adult pollock in trawls fished in the 0–60 m layer of the water column

Table 1. Estimated total consumption (millions) of juvenile salmon by nine taxonomic and three functional groups (see Willette, 2001; this volume p. 110) of fish predators in Prince William Sound during May–June

Taxonomic group	Predator		Predator consumption of salmon (millions)		
	Density	Abundance	Low	Point	High
Planktivores					
Herring	0.1030	186.23	14.60	146.02	321.24
Pollock (age 3+)	0.0025	22.00	43.56	108.90	174.24
Pollock (age 1–2)	0.0280	5.00	20.24	20.24	20.24
Pelagic rockfishes	0.0040	0.72	4.32	4.32	4.32
Salmon	0.0017	3.06	9.24	9.24	9.24
Total	0.1392	217.01	91.96	288.71	529.28
Piscivores					
Other gadids	0.0280	5.00	134.57	224.28	358.85
Trout	0.0001	0.16	0.77	7.74	11.61
Total	0.0281	5.16	135.34	232.02	370.46
Invertebrate feeders					
Benthic fishes	0.0140	2.59	10.53	13.16	15.79
Demersal rockfishes	0.0040	0.72	0.66	0.66	0.66
Total	0.0180	3.31	11.18	13.82	16.45

This analysis of field data was intended only to provide order-of-magnitude estimates of losses of salmon to various predator taxonomic groups and identify those groups that could be neglected in our numerical modelling. Total consumption of salmon was calculated using estimates of daily individual predator consumption of salmon provided by Willette (2001; this volume p. 110; Table 9), as well as estimates of predator density (number/m^2) and abundance (millions). The probable range of predator consumption of salmon was calculated by multiplying the point estimate of predator abundance by the observed percent deviation of mean catch per net set among years (1995–97) for each predator group (Willette, 2001; this volume; Table 7). Predator functional groups were based upon their diet compositions (Willette, 2001; this volume).

declined seasonally (Willette, 2001; this volume p. 110). Acoustic data indicated that adult pollock migrated deeper in the water column as the surface layer warmed and densities of large copepods declined in July (Thomas et al., 1998). Among the nearshore fishes, relative abundances of trout increased by a factor of 10 from early May to June, whereas immature pollock abundances increased by about a factor of 2 (Willette, 2001; this volume p. 110).

Simulation of predator–prey interactions: model validations

The diet composition and growth of juvenile salmon predicted by our numerical model was generally similar to estimates of these parameters from field studies conducted in 1994 and 1995. The model accurately predicted a switch from large copepods to 'other zooplankton' (mostly pteropods) occurring near the beginning of June in both years (Fig. 6b,d), but it did not predict relatively high consumption of small copepods (mostly *Pseudocalanus*) during early June 1994 and May 1995 (Fig. 6c). Cox and Stuart tests indicated a significant trend in model residuals for 'other zooplankton'

consumed by juvenile salmon, while Wilcoxon signed rank tests indicated mean residuals were significantly different from zero for small copepods consumed by juvenile salmon.

More importantly, simulated juvenile salmon growth was not significantly different from observed growth for 16 CWT groups of juveniles released from WHN Hatchery in both 1994 and 1995. Although there was no significant trend in model residuals, simulated body weights tended to be less than observed weights later in the season (Fig. 6a). This could have been caused by an inaccuracy in the growth model, but the effect of size-selective predation on observed size distributions within CWT groups was a likely explanation. Our model could not reproduce this effect, because only the mean body weight for the salmon in each CWT group was available as a model input.

The diet composition of adult pollock and size selectivity of prey predicted by our numerical model were also generally similar to estimates of these parameters from field studies. Although observed consumption of juvenile salmon was less than predicted consumption (Fig. 7b),

Figure 6. Comparison of observed and model predicted diet composition and growth for CWT juvenile salmon released from Wally H. Noerenberg Hatchery in 1994 and 1995. Mean square errors (MSE) were calculated to evaluate model fit. W-test and associated P-values indicate whether mean deviations between predicted and observed values were different from zero (Wilcoxon signed rank tests). C-test and associated P-values indicate whether there was a significant trend in the deviations between predicted and observed values over time (Cox and Stuart test). Only field data from the first tag group released in each year are indicated for comparison with simulated growth. Zooplankton densities are indicated for *Neocalanus* spp. stage 4 (thin solid lines), *Neocalanus* spp. stage 5 (heavy solid line), *Pseudocalanus* spp. (thin dashed lines), and pteropods (heavy dashed lines).
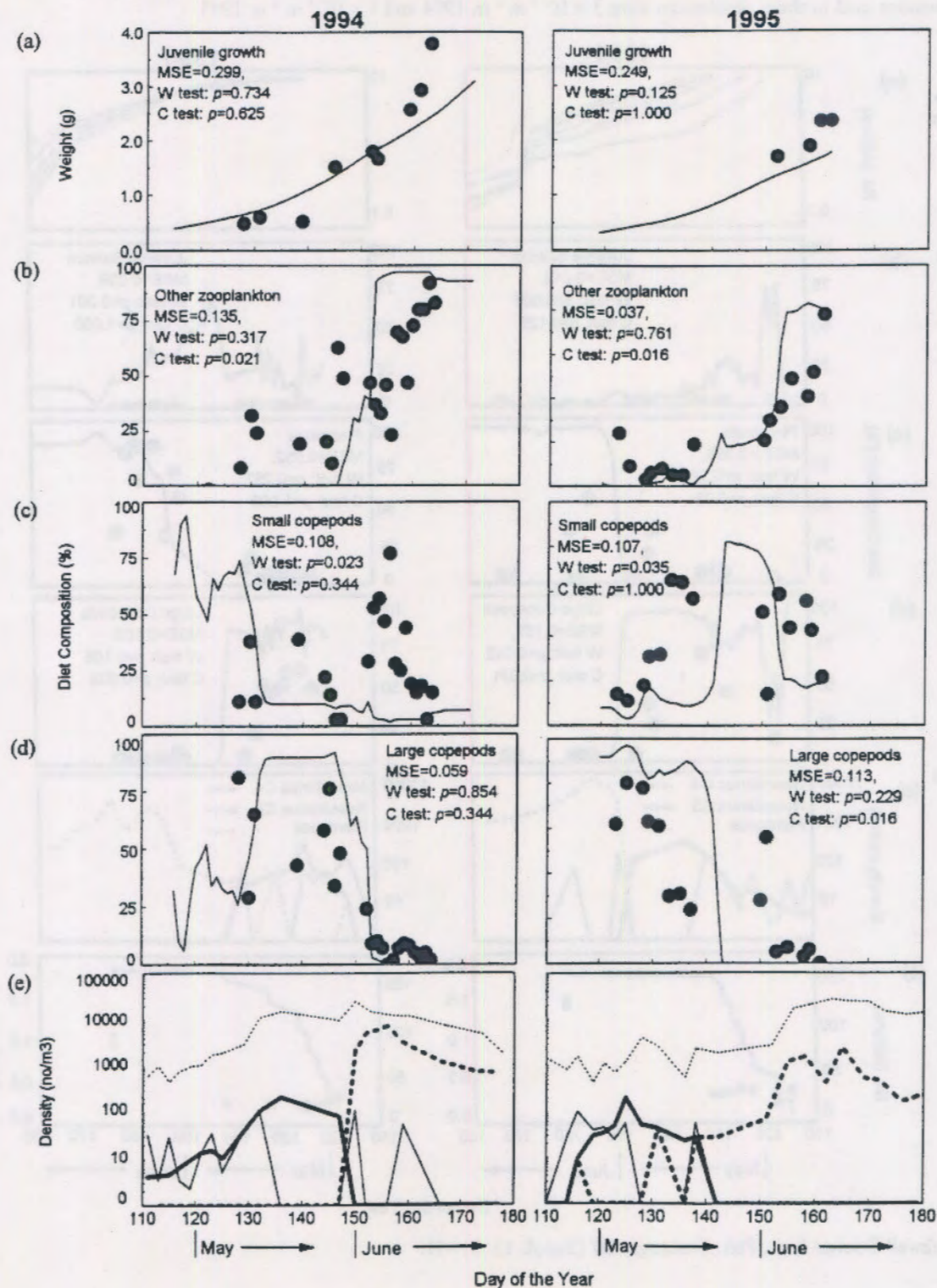
Figure 7. Comparison of observed and model predicted diet composition for adult walleye pollock along the migratory pathway of juvenile salmon released from Wally H. Noerenberg Hatchery in 1994 and 1995. Juvenile salmon release schedules, seasonal changes in the zooplankton bloom, and simulated abundance trajectories for multiple releases of juveniles from this hatchery are also indicated. The mean wet weight of juvenile salmon in each release group (solid squares) and the cumulative number of salmon released (solid line) are indicated in the lower panel. Mean square errors (MSE) were calculated to evaluate model fit. W-test and associated P-values indicate whether mean deviations between predicted and observed values were different from zero (Wilcoxon signed rank tests). C-test and associated P-values indicate whether there was a significant trend in the deviations between predicted and observed values over time (Cox and Stuart test). Adult pollock densities used in these simulations were 3×10^{-3} m^{-2} in 1994 and 1×10^{-3} m^{-2} in 1995.
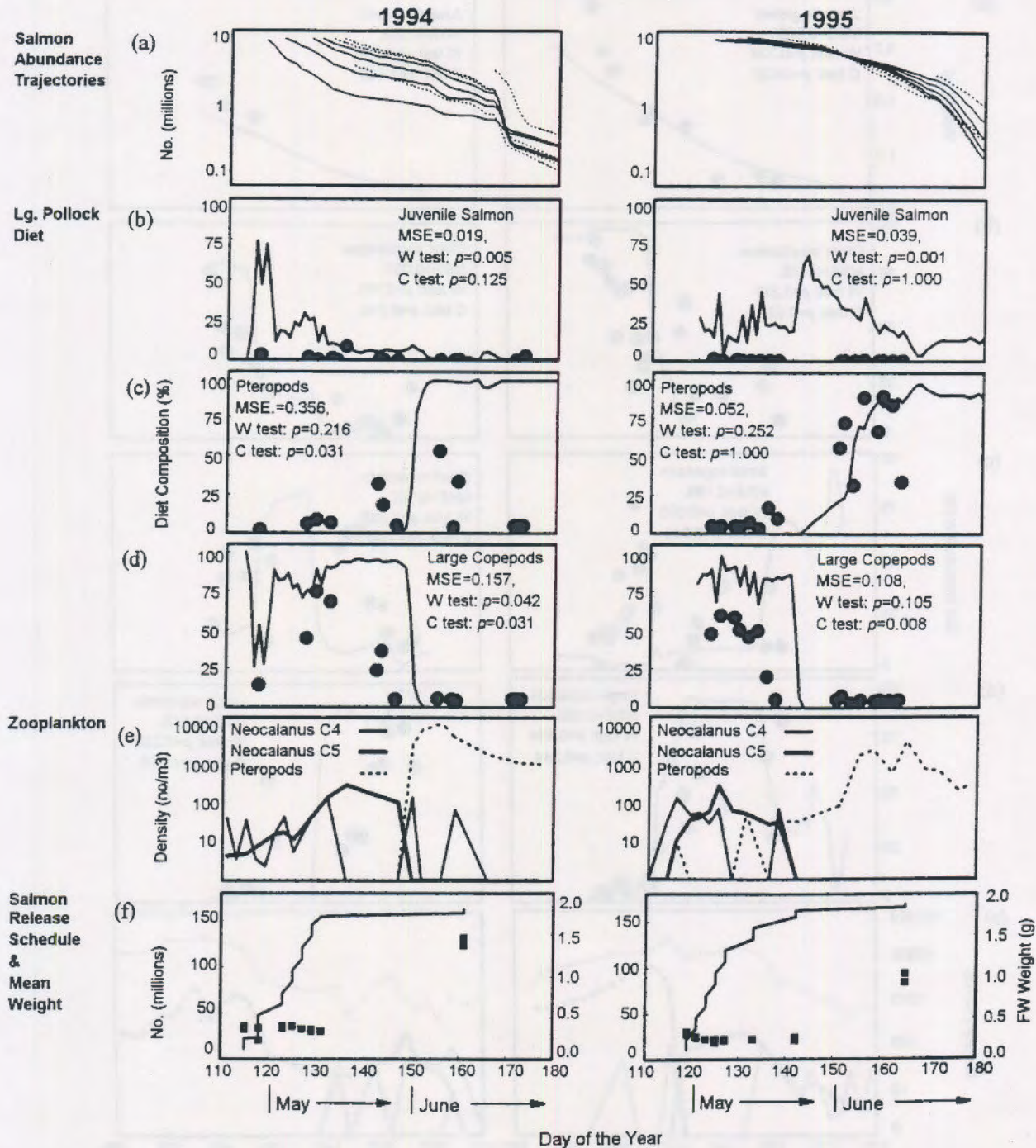
Figure 8. Length distributions of juvenile salmon consumed by adult and immature pollock predicted by our foraging-physiology-dispersion model (solid lines) compared with estimates from field studies (dashed lines), 1995. Kolmogorov–Smirnov tests indicated that simulated and observed length distributions of salmon consumed by adult pollock were significantly different, but there was no difference for immature pollock (*P* = 0.05).

Juv. Salmon Length (cm)
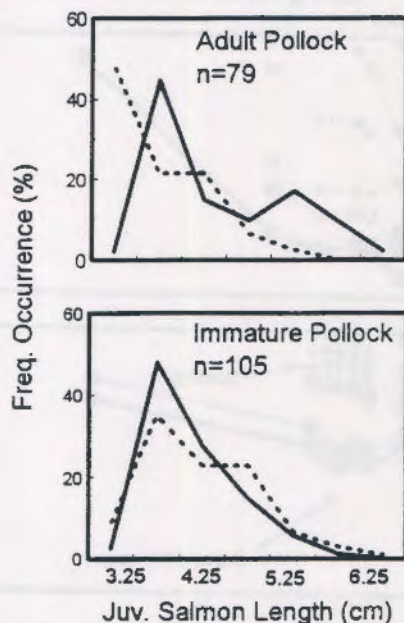
the simulation exhibited an observed switch from large copepods to pteropods by adult pollock occurring near the beginning of June in both years (Fig. 7c,d). Model residuals exhibited a significant temporal trend for large copepods consumed by adult pollock. The model tended to overestimate actual consumption of large copepods during the copepod bloom and underestimate consumption after the bloom. Kolmogorov–Smirnov tests indicated that simulated and observed length distributions of salmon consumed by adult pollock were significantly different, but there was no difference (*P* = 0.05) for immature pollock (Fig. 8). This validation analysis was an important test of model performance, because simulated prey length distributions resulted from the capture probability and optimized prey selection functions in the model (Equation 2), as well as the timing of predation losses (Fig. 7a) in relation to simulated juvenile growth (Fig. 6a).

Comparison of actual survival (S_{ret_i}, release to adult return) with simulated survival of CWT juvenile salmon to day of year 180 (S_{juv_i}) indicated that patterns of survival by date of release were accurately predicted by the model for pink salmon released from the Armin F. Koernig (AFK) and WHN Hatcheries in 1994 and 1995 (Fig. 9). Cox and Stuart tests indicated no significant

trend in model residuals ($Resd = \ln S_{juv_i} - \ln S_{ret_i}$) by date of release for any of the four cases. The time evolution of simulated survivals plotted by date of release indicated: (i) for CWT groups released from WHN in May 1994–95 (Fig. 9b,d, right panel), a minimum in survival by date of release was established in late June (after day 165); (ii) for CWT groups released from AFK Hatchery in May 1994 (Fig. 9a, right panel), a strong pattern of increasing survival by date of release was established early in the juvenile period; and (iii) for CWT groups released from AFK Hatchery in May 1995 (Fig. 9c, right panel), a maximum in survival by date of release was established early in the juvenile period. Examination of simulated abundance trajectories for these CWT groups (Figs 7a and 10a,d) indicated several episodes of high mortality that largely established the observed patterns of survival by date of release.

Simulation of predator–prey interactions: Analysis of ecological processes

When the sheltering and satiation thresholds were plotted against salmon length, three differences between the two predators were apparent (Fig. 11). First, the satiation threshold occurred at higher salmon densities for adult pollock than immature pollock; second, the sheltering and satiation thresholds were much more dependent on salmon length for immature than adult pollock; and, third, the satiation threshold was very near the sheltering threshold for adult pollock, but it was much lower than the sheltering threshold for immature pollock. Thus, in a simulated system dominated by immature pollock, salmon could benefit from both predator satiation and zooplankton sheltering over a fairly broad range of salmon densities, but this would not be the case in a system dominated by adult pollock (Fig. 11). Also, since adult pollock enter a linear feeding mode at much higher salmon densities, salmon would be much more vulnerable to predation in a system dominated by these predators.

The degree of sheltering by zooplankton differed among zooplankton types, and the degree of sheltering was dependent on both predator and salmon sizes. Consumption of salmon was reduced to 20% of the level before the transition when densities of *Neocalanus* stage 5 exceeded 100 m^{-3} (Fig. 12). The same reduction in salmon predation required densities exceeding 200 m^{-3} for *Neocalanus* stage 4 or pteropods as alternative prey (Fig. 12). As juvenile salmon increased in size, the degree of sheltering by zooplankton became more dependent on salmon size than zooplankton density, because the degree of sheltering was in part a function of the handling time of salmon per unit mass captured (Equation 5). In a system dominated by immature

Figure 9. Left panel: Survival of multiple (*i*) CWT groups of pink salmon (S_{ret}, release to adult return, see Figure 5) by their date of release (abscissa) from Wally H. Noerenberg & Armin F. Koernig Hatcheries, 1994–95. Right panel: Time evolution (downward arrows indicate time) of the simulated survivals of each CWT group to day of the year 120, 130, 140, and 150 after release (thin dashed lines) and survivals to days 160, 170 (thin solid lines) and 180 (S_{juv_i}, heavy solid lines) after release. Model performance was evaluated by comparing the patterns of survival by date of release between S_{ret} and S_{juv_i}. Cox and Stuart tests indicated no significant trend in model residuals ($Resd = \ln S_{juv_i} - \ln S_{ret}$) by date of release for any of the four cases.
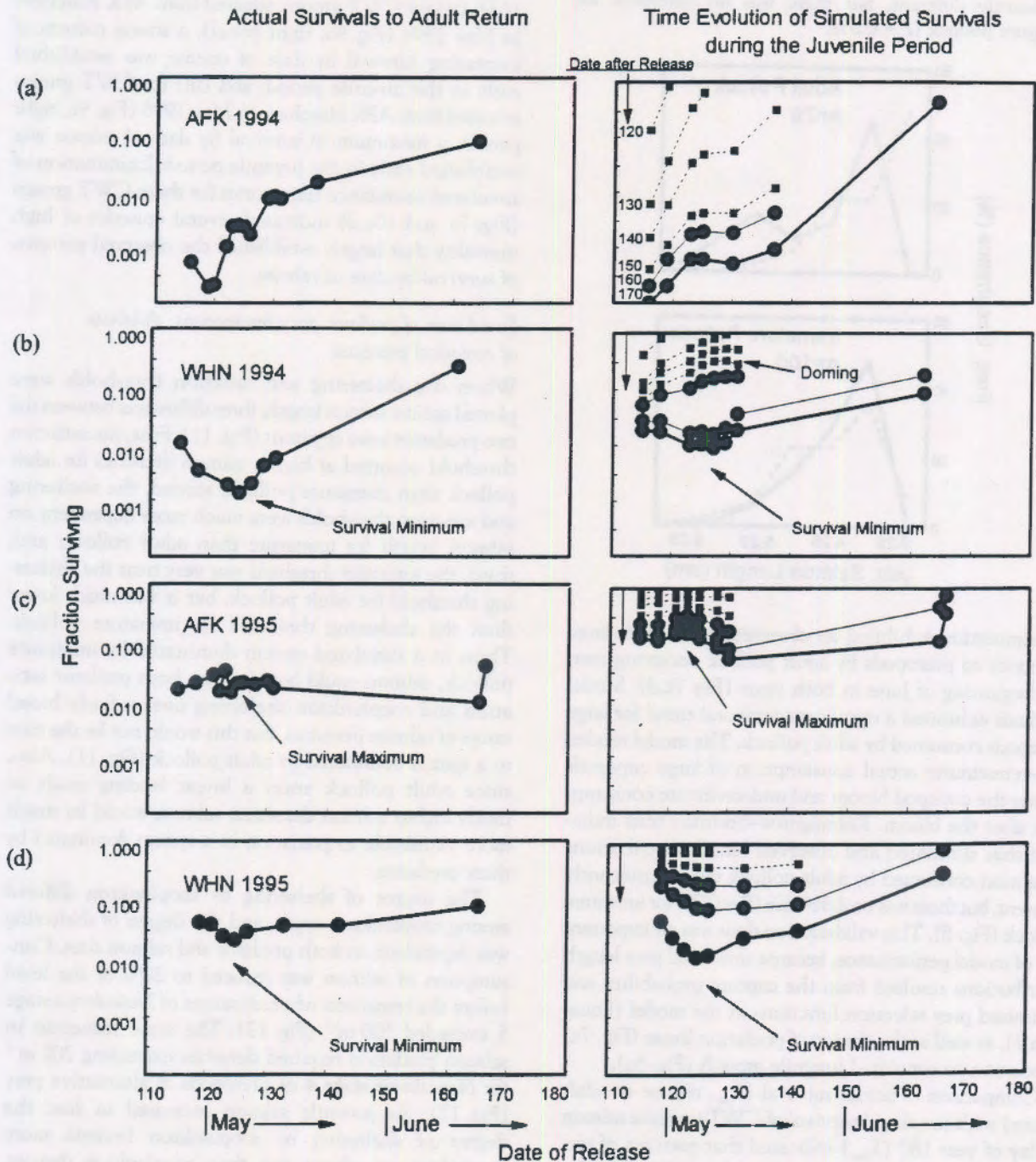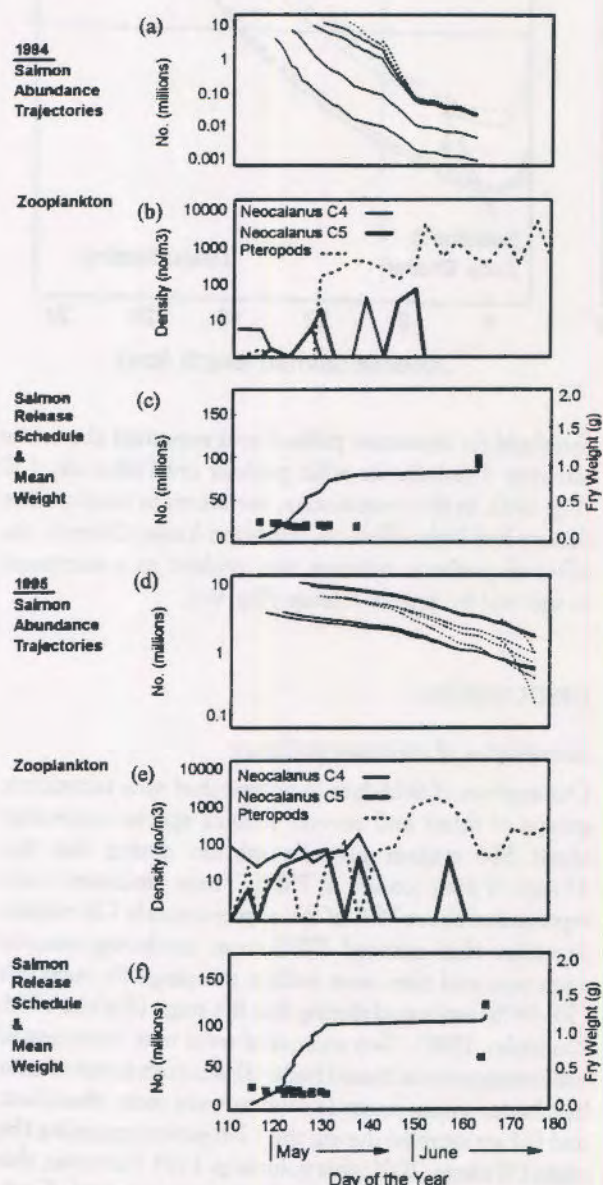
Figure 10. Juvenile salmon release schedules, seasonal changes in zooplankton bloom, and simulated abundance trajectories for multiple releases of juveniles from Armin F. Koernig Hatchery, 1994–95. The mean wet weight of juvenile salmon in each release group (solid squares) and the cumulative number of salmon released (solid line) are indicated in the lower panel. The adult pollock density used in the 1994 simulation was 2×10^{-3} m^{-2}. In the 1995 simulation, predator densities were 8×10^{-4} m^{-2} for adult pollock and 5×10^{-3} m^{-2} for immature pollock.

1994
Salmon
Abundance
Trajectories

Zooplankton

Salmon
Release
Schedule
&
Mean
Weight

1995
Salmon
Abundance
Trajectories

Zooplankton
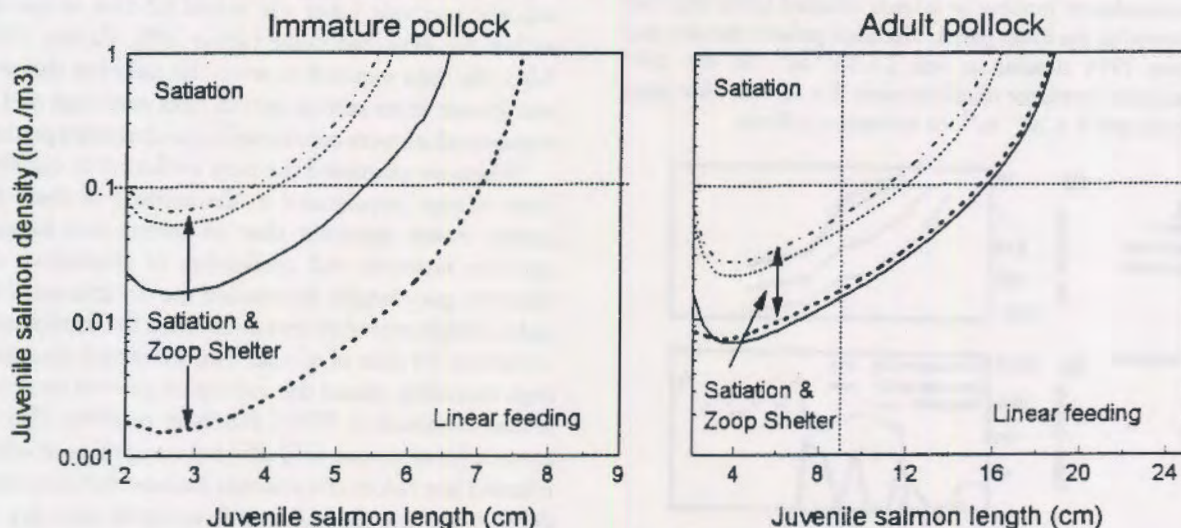
Salmon
Release
Schedule
&
Mean
Weight

pollock, the degree of sheltering by zooplankton became more size dependent when salmon lengths exceeded 5–6 cm, whereas in a system dominated by adult pollock, a similar effect would not occur until salmon lengths exceeded 14–18 cm.

When predators were satiated, the relative production of predator and prey populations determined whether prey populations crashed or bloomed (Fig. 13). This analysis indicated the role of high salmon growth rates as one means to avoid a population crash and achieve survivals (over the initial 60 days of sea life) within the expected range (about 20%, Parker, 1968). Also, the time required to reach the satiation threshold was shorter when salmon growth rates were high and immature pollock were considered as the dominant predator.

When we examined the time evolution of our simulated salmon populations in the context of these processes, it was apparent that an interaction between predator satiation and availability of alternative zooplankton prey largely determined the occurrence of episodes of high mortality that established the final patterns of survival by date of release. Two simulated episodes of high mortality caused the pattern of survival by date of release observed at WHN Hatchery in 1994. The first episode (prior to day 135) affected two groups of salmon released just before the seasonal increase in *Neoocalanus* density, and the second episode occurred after day 165 (Fig. 7a). Both episodes of high mortality occurred because salmon densities dropped below the satiation threshold for adult pollock, and zooplankton densities were insufficient to shelter them from the effects of linear feeding. Mortality during the second episode was greatest among salmon released between days 120–130. The cumulative abundance of salmon increased from 50 to 150 million during this period creating a high-density mass of juveniles moving down the migratory pathway. Initially, individuals at the centre of this mass benefited from predator satiation. This effect was evident as a 'doming' of the survivals plotted by date of release (Fig. 9b, right panel). Then after day 165, salmon densities dropped below the satiation threshold. Predation losses then became a function of salmon density causing higher losses among high-density groups of salmon produced from earlier consecutive releases. The effect of this process was evident as a minimum in survival by date of release (Fig. 9b).

Simulated survivals of juveniles released from WHN Hatchery in 1995 were somewhat different from 1994, because the juvenile release schedule and the evolution of the zooplankton bloom differed. Again, several net pens were released within a few days of each other in early May (days 120–130), but unlike the previous year these releases occurred during the peak of the *Neocalanus* bloom (Fig. 7e,f). The simulated mortality of these fish was initially very low, but on day 140 the *Neocalanus* bloom declined, and several days elapsed before the pteropod bloom began. During this period, simulated pollock diet composition indicated high consumption of salmon

Figure 11. Threshold salmon densities at which immature and adult pollock transition from feeding exclusively on salmon to feeding on alternative zooplankton prey in relation to salmon length and density. Line types indicate different curves for alternative zooplankton prey: *Neocalanus* stage 4 (dotted line), *Neocalanus* stage 5 (dot-dashed line), pteropod (solid line). The vertical line on the plot for adult pollock emphasizes the difference in scale between the two plots. The horizontal lines are a reference to emphasize the difference in the shape of the curves between the two predators. The heavy dashed line indicates the threshold at which pollock transition from satiation to a linear feeding mode (at 6 °C).

at a time when no field sampling was conducted. But the simulated population did not crash because low mortality during the previous 20 days had kept salmon densities above the satiation threshold. This situation changed after day 170 when salmon densities dropped below the satiation threshold, and pteropod densities were insufficient to shelter juveniles from predation. An episode of high mortality resulted (Fig. 7a) causing a minimum in survival by date of release associated with high-density groups of salmon produced from earlier consecutive releases (Fig. 9d).

The effects of low salmon densities and a weak zooplankton bloom were evident in the simulation of AFK Hatchery releases in 1994. In this case, salmon densities were generally below the predator satiation threshold, because small numbers were released over a prolonged period (Fig. 10a). In this system state, zooplankton densities sufficient to shelter juveniles from predation were necessary to avoid a population crash, so variations in zooplankton density largely modulated predation losses. Periods of high juvenile mortality were evident when zooplankton densities were low prior to day 135 and between days 140–150. Overall, survivals were very poor particularly for the early release groups exposed to predation for a longer time (Fig. 9a).

The simulation of AFK Hatchery releases in 1995 demonstrated the effect of immature pollock as the dominant predator and a strong zooplankton bloom. In this case, salmon densities never dropped below the satiation

threshold for immature pollock and remained above the satiation threshold for adult pollock until after day 150 (Fig. 10d). In this system state, variations in zooplankton density had little effect on predation losses. Overall, the effect of predator satiation was evident as a maximum in survival by date of release (Fig. 9c).

DISCUSSION

Identification of important predators

Our analyses of field data indicated that nine taxonomic groups of fishes and several seabird species consumed about 546 million juvenile salmon during the first 45 days of their sea life in PWS. These predation losses represented about 75% of the approximately 726 million juveniles that entered PWS from bordering streams each year and thus were within the range for survivals (53–94%) estimated during this life stage (Parker, 1968; Karpenko, 1998). Two sources of error may have caused our estimates to be biased high: (i) we often sampled near hatcheries where juvenile salmon were more abundant; and (ii) we sampled during the 12-h period spanning the night (Willette, 2001; this volume p. 110). However, this bias may have been offset by errors in our method of estimating predation losses from stomach content analysis, because the mass of salmon consumed was underestimated due to digestion prior to sample analysis. Comparisons of predation loss among predator groups were

Figure 12. Reduction in individual consumption of salmon by immature and adult pollock in proportion to their consumption of salmon prior to a transition to feeding on alternative zooplankton prey (contour lines) plotted in relation to salmon length and the density of alternative zooplankton prey.
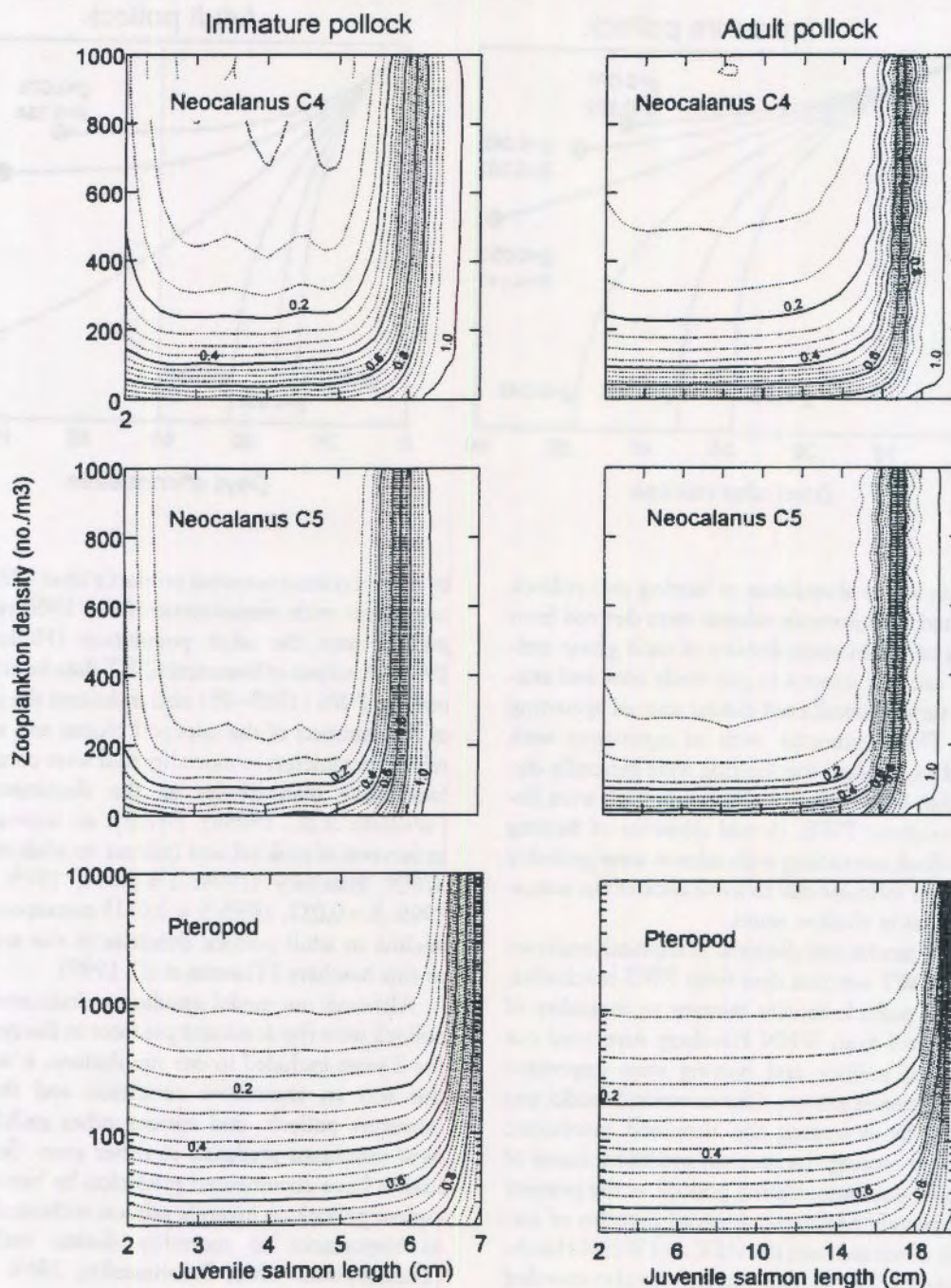

probably affected little by either of these sources of error.

Comparison of total consumption of juvenile salmon among predator groups was dependent on our predator abundance estimates and assumptions regarding the degree of overlap between predator and prey distributions. Although stomach analyses indicated that individual herring and adult pollock consumed the smallest numbers of salmon, total predation losses to these two predators were likely high due to their high abundance.

Figure 13. Theoretical salmon population trajectories assuming predator satiation and given the range of salmon growth rates (*g*, % body weight per day) typically observed in Prince William Sound. Survivals (*S*) over the initial 60 days of sea life are indicated for cases where the final population size was greater than zero. Solid dots indicate when predators transition from satiation to a linear feeding mode.
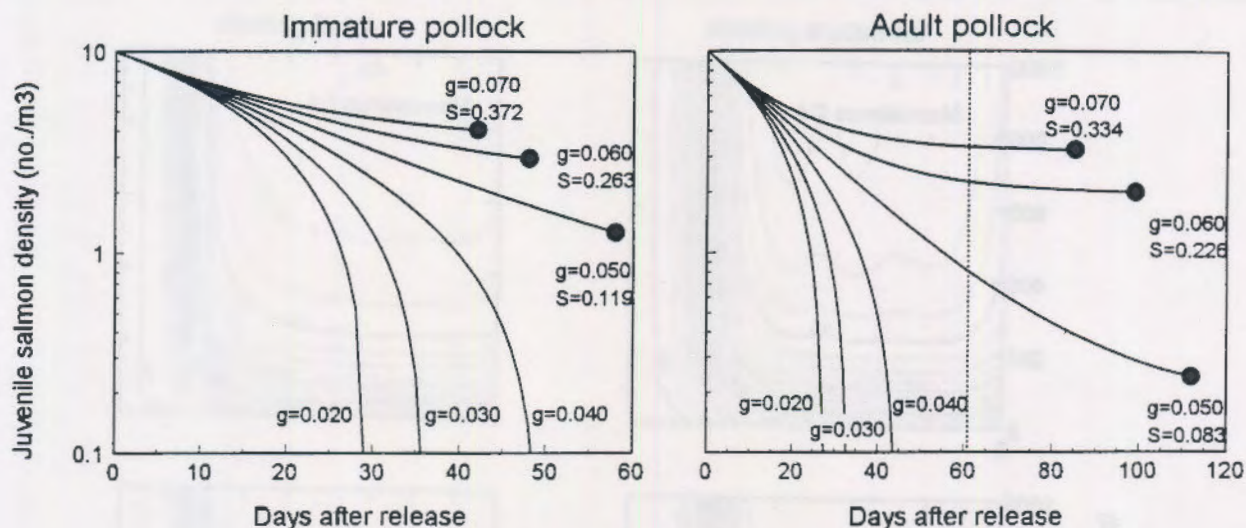
Our estimates of the abundance of herring and pollock that interacted with juvenile salmon were derived from comparisons of the biomass density of each group estimated from acoustic surveys in our study area and estimates from surveys conducted during annual spawning migrations. These estimates were in agreement with each other if we assumed that herring were generally distributed within 1 km of shore and adult pollock were distributed throughout PWS. Actual densities of herring and adult pollock interacting with salmon were probably higher than our estimate due to avoidance of the acoustic survey vessel in shallow water.

Numerical model simulations, statistical analyses of historical CWT survival data from PWS hatcheries, and trends in pollock density relative to mortality of juveniles released from WHN Hatchery supported our conclusion that pollock and herring were important predators on juvenile salmon. Our numerical model was a useful tool for evaluating the sizes and taxonomic groups of fishes causing the greatest predation losses of salmon. Model simulations using pollock as the primary predator accurately predicted observed patterns of survival by date of release from the AFK and WHN Hatcheries in 1994–95 (Fig. 9). Our simulations also revealed the signature of a large planktivore predator (adult pollock) in the system, i.e. a minimum in survival of salmon by date of release associated with multiple pen releases (Fig. 9b,d). Examination of patterns of survival by date of release over the full CWT data set (Willette *et al.*, 1999b) indicated that a minimum in survival of salmon

by date of release occurred primarily after 1992. This was consistent with recruitment of the 1988 year class of pollock into the adult population (Hollowed *et al.*, 1996). Analyses of historical CWT data from four hatcheries in PWS (1989–95) also indicated the importance of the duration of the copepod bloom and several size-related parameters to mortality that were consistent with facultative planktivores as the dominant predator (Willette *et al.*, 1999a). Finally, an increasing trend in survival of pink salmon (release to adult return) from WHN Hatchery (1994: $S = 0.014$, 1995: $S = 0.031$, 1996: $S = 0.037$, 1997: $S = 0.071$) corresponded with a decline in adult pollock densities in the area adjacent to this hatchery (Thomas *et al.*, 1998).

Although our model simulations indicated that adult pollock were the dominant predator in the system during the 2 years included in our simulations, it is likely that this was an anomalous condition and that herring, immature pollock, and various other gadids were the most important predators in other years. Several other studies have documented predation by herring and immature pollock on juvenile salmon without determining its importance to mortality during early sea life (Thorsteinson, 1962; Bakshtanskiy, 1964; Armstrong and Winslow, 1968).

Simulation of predator–prey interactions:
model validation

Accurate simulation of patterns of survival by date of release for pink salmon released from AFK and WHN

Hatcheries (1994–95) demonstrated that the structure of our numerical model (Figs 3–5) provided an effective representation of the responses of the interacting trophic groups (Fig. 2) to their simulated space-time circumstances. Availability of survival estimates for multiple groups of CWT juveniles released at various times, densities, and sizes greatly increased the efficacy of our model validations, because the structure of the data limited the number of sets of conditions that could have produced the observed outcome.

Our comparison of observed and simulated consumption of salmon by adult pollock suggested an apparent failure of the model because simulated consumption was higher than observed (Fig. 7b). However, a thorough assessment of model performance must consider that the model only simulated the diet of pollock that interacted with salmon. Conceptually, the model collapsed the actual three-dimensional system into a single dimension in which all pollock present at a specific location encountered salmon as they migrated from the hatcheries. In the actual system, only a small fraction of the pollock present in our survey area actually encountered salmon. The majority of our field samples of adult pollock were collected with a mid-water trawl fished at depths ranging from 10 to 60 m in the passages. Samples collected in this manner represented the entire stock present in the survey area, not solely those pollock interacting with juvenile salmon. This effect was not evident in comparisons of observed and simulated consumption of zooplankton, because nearly every pollock present in the survey area encountered these more ubiquitous preys.

To a lesser extent patchiness in zooplankton distributions contributed to differences between observed and simulated diets of salmon and pollock, because the zooplankton sample data used to drive the model were collected at sites several kilometres from our field study sites. The model was driven by zooplankton data obtained from biweekly samples collected at a single station adjacent to each hatchery. Samples used to estimate diet composition for model validation were sometimes collected at sites 10–20 km distant from the zooplankton sample station adjacent to WHN Hatchery. Zooplankton data collected at stations adjacent to hatcheries were used to drive the model, because they provided a time series of observations from a single site with a consistently high sampling frequency. Zooplankton samples collected along the salmon migratory pathway described the spatial distribution of the plankton, but they did not adequately represent the evolution of the zooplankton bloom at each location, because the sampling frequency at each station was too sparse.

Simulation of predator–prey interactions: analysis of ecological processes

Our numerical modelling suggested two strategies that juvenile salmon can employ to reduce predation losses, but high macrozooplankton densities are necessary for success in both strategies. The first strategy called 'predator swamping' involved the formation of high-density aggregations of salmon to satiate predators. The second strategy called 'zooplankton sheltering' involved dispersing sufficiently to cause predators to switch to planktivory. The predator-swamping strategy can only be successful if zooplankton densities are sufficient to support high juvenile growth rates in high-density aggregations of salmon (Fig. 13). The zooplankton-sheltering strategy can only be successful if zooplankton densities are sufficient to shelter salmon from predation (Fig. 12 and 14).

The two strategies are not mutually exclusive; in fact an interaction between them is probably common. This was the case in our simulations of WHN Hatchery releases during both years used for model validation. Examination of the time series plots from these simulations suggested that the satiation threshold was often reached later in the juvenile period when pteropods were the only zooplankton occurring in sufficient densities to shelter juveniles from predation. Thus, the June pteropod bloom may be very important in sheltering salmon from predation, because it occurs at a time when salmon densities are approaching the satiation threshold.

But closer inspection of the spatial variation in our model simulations also revealed salmon densities below

Figure 14. Relationship between the mean percent of the diet composed of nekton and the biomass of large calanoid copepods for herring (solid squares), immature pollock (solid circles) and adult pollock (open circles). Data from 1994 to 1996 (Willette *et al.*, 1999a).
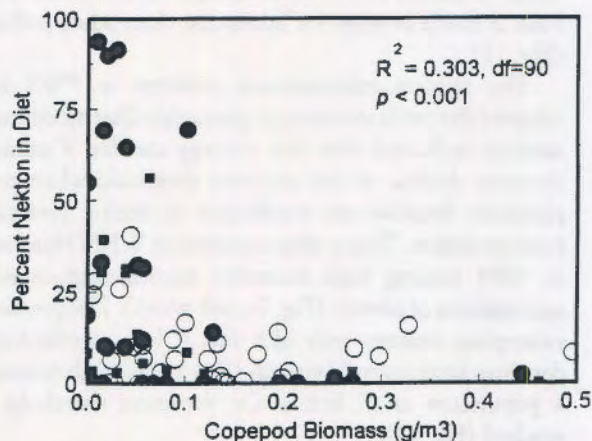
the satiation and sheltering thresholds at various locations during the entire juvenile period (Patrick *et al.*, 2001). Salmon densities were usually above the sheltering threshold in the centre of aggregations, but the sheltering threshold was eventually reached as salmon densities declined away from the centre of aggregations. Thus, the spatial variation in salmon densities likely results in a heterogeneous distribution of predation events in both space and time. Given this distribution, field samples collected and averaged over relatively large spatial scales could not adequately represent predation losses with any practical level of sampling effort. Also, the occurrence of salmon in predator stomachs should be less frequent and predation events more contagiously distributed when zooplankton densities (particularly *Neocalanus*, stage 5) are high because as salmon densities decline away from the centre of aggregations and the sheltering threshold is reached, predation losses of salmon abruptly decrease (Fig. 12). The converse should be true when zooplankton densities are lower, i.e. salmon should occur more frequently in predator stomachs and the distribution of predation events should be more homogeneous. These patterns were observed in our field data, but they were confounded by dispersion of salmon from shallow nearshore habitats when copepod densities declined (Willette, 2001; this volume p. 110).

The dominance of adult pollock in the system produces a state in which salmon may be more vulnerable to a population crash. When adult rather than immature pollock are the dominant predator in the system, the satiation threshold occurs at salmon densities nearly an order of magnitude higher (Fig. 11). The transition to a linear feeding mode at higher salmon densities can cause higher proportional predation losses to occur earlier in the juvenile period, if zooplankton densities are insufficient to shelter juveniles from predation. Also, there is a zone of salmon densities above the satiation threshold and below the sheltering threshold in which predation losses of salmon can be reduced by both processes. This zone is much broader for immature than adult pollock (Fig. 11).

The salmon enhancement industry in PWS has adopted the predator-swamping strategy. Our model simulations indicated that this strategy can fail if salmon densities decline to the satiation threshold when zooplankton densities are insufficient to shelter juveniles from predation. This is what occurred at WHN Hatchery in 1994 causing high mortality among high-density aggregations of salmon (Fig. 7a, left panel). The predator swamping strategy may also fail if low zooplankton densities limit juvenile growth (Fig. 15) enough to cause a population crash before the satiation threshold is reached (Fig. 13).

Figure 15. Growth rates (% body weight day^{-1}) of hatchery-reared coded-wire tagged juvenile pink salmon in relation to mean zooplankton density during the initial 30 days of marine residence (Willette *et al.*, 1999b) for groups composed of less than 20 million (solid circles and line) and greater than 20 million individuals (open circles and dashed line).
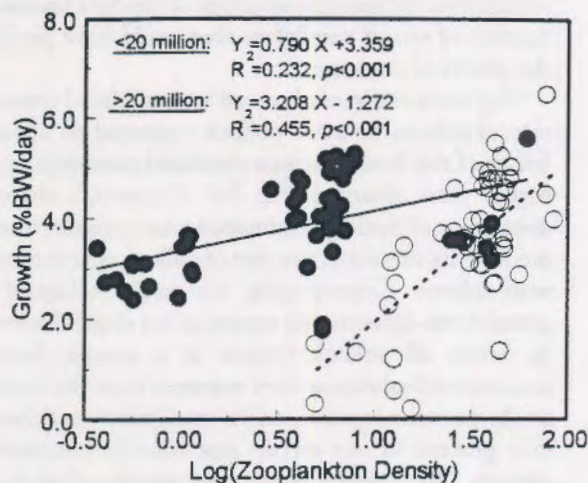
Synthesis and evaluation of hypotheses

Our prey-switching hypothesis was supported by analyses of stomach contents of walleye pollock and herring, statistical analyses of survival data, and numerical model simulations (Table 2). Individual consumption of juvenile fishes by these two facultative planktivores was inversely correlated with the mean biomass of large calanoid copepods (Willette *et al.*, 1999a). The diets of these predators were dominated by large calanoid copepods (60–90% of total stomach content weight) during the copepod bloom. After the bloom, they switched to alternative nekton prey including juvenile salmon when the biomass of large copepods declined below about 0.2 g m^{-3} (Fig. 14). An analysis of historical CWT survival data also supported our prey-switching hypothesis. Willette *et al.* (1999a) found that mortality of pink salmon was negatively correlated with the duration of the zooplankton bloom during the juvenile lifestage ($P = 0.013$), as well as with juvenile growth rate ($P < 0.001$), juvenile body weight at release ($P < 0.001$), and the number of juveniles released ($P < 0.001$). The importance of the duration of the zooplankton bloom and these size-related parameters to mortality was consistent with facultative planktivores as the dominant predator and sheltering of juveniles from predation by planktivores.

Our model simulations were consistent with these field data, but they also revealed much more about the nature of these ecological processes. Consistent with field observations, simulated predation losses of salmon

Table 2. Summary of analytical methods, and dates/areas in Prince William Sound (PWS) where data were collected to evaluate each hypothesis. Areas generally indicated by location of nearest hatchery (see Fig. 1): Armin F. Koernig (AFK), Wally H. Noerenberg (WHN), Cannery Creek (CCH), and eastern PWS (E)

Conclusion	Method	Data type	Area	Year
Prey-switching hypothesis	Statistical analysis of consumption of fish by pollock and herring	Stomach content analysis predators	AFK, WHN, CCH	1994–1996
		Zooplankton biomass	AFK, WHN, CCH	1994–1996
		Ocean temperature	AFK, WHN, CCH	1994–1996
	Statistical analysis of survival	Same as above		
	Numerical model simulations	Same as above		
Refuge-dispersion hypothesis	Statistical test of nearshore vs. offshore difference in zooplankton density and juvenile feeding rate	Zooplankton biomass nearshore and offshore	WHN	1995
		Stomach content analysis of juvenile salmon nearshore and offshore	WHN	1995
	Statistical test of CWT juvenile growth vs. number juvenile released	CWT juvenile growth rate	PWS	1989–1994
		Number of juveniles released	PWS	1989–1994
		Zooplankton biomass	PWS	1989–1994
	Statistical test of juvenile condition vs. juvenile density	Whole body energy content	WHN, CCH, E	1995–1997
		Juvenile salmon relative abundance	WHN, CCH, E	1995–1997
	Statistical analysis of consumption of juvenile salmon by predators and offshore juvenile abundance	Stomach content analysis predators	WHN, CCH, E	1995–1997
		Net sample – cpue*	WHN, CCH, E	1995–1997
		Juvenile salmon length	WHN, CCH, E	1995–1997
Size-refuge hypothesis	Statistical analysis of consumption of juvenile salmon by predators	Stomach content analysis predators	WHN, CCH, E	1995–1997
		Juvenile salmon length	WHN, CCH, E	1995–1997

*cpue: catch per unit effort.

were reduced to 20% of the level before the transition to planktivory (Fig. 12b) when densities of *Neocalanus* stage 5 exceeded 100 m^{-3} ($\sim 0.2 \text{ g m}^{-3}$). However, the simulations also showed that zooplankton sheltering was not important if salmon densities were above the sheltering and satiation thresholds (Fig. 11). As salmon densities declined below the sheltering threshold, predation losses of salmon could be reduced if zooplankton densities were sufficient to shelter salmon. But, zooplankton sheltering was most important when salmon densities declined below the satiation threshold, because potential predation losses were much greater then. In our simulations of hatchery releases, the satiation threshold was often reached in June, when pteropods were the only zooplankton occurring at sufficient densities to shelter salmon from predation. Our simulations also suggested that zooplankton sheltering may be more important to wild salmon, because this salmon stock enters the sea at much lower densities. If their densities decline below the satiation threshold earlier in the juvenile period, zooplankton densities sufficient to shelter them from predation would be necessary to reduce their predation losses.

Our refuge-dispersion hypothesis was supported by analysis of predator stomach contents, relative abundances of juvenile salmon in nearshore and offshore habitats in relation to macrozooplankton biomass, differences in macrozooplankton biomass and species composition between nearshore and offshore habitats, and evidence of density-dependent growth (Fig. 15). The biomass of large copepods and the proportion of juvenile salmon diets composed of large copepods were higher offshore than nearshore (Willette, 2001; this volume p. 110). Juvenile salmon dispersed from nearshore habitats when the biomass of large copepods (primarily *Neocalanus* spp.) declined. When salmon dispersed offshore, mean daily individual predator consumption of salmon increased by a factor of 5, and the number of salmon consumed was inversely related to salmon size.

Salmon probably foraged in risky offshore habitats to maintain high feeding rates and avoid later size-dependent predation. Although daily individual predator consumption of salmon was generally not different between early May and June (Willette, 2001; this volume p. 110), salmon mortality likely increased by nearly an order of magnitude during this period, because the number of salmon available to predators was declining due to earlier predation losses. This process was evident in our model simulations as an increasing negative slope in population trajectories (Figs 7a, 10a,d and 13). An increasing probability of predation coupled with negative size-dependent vulnerabilities of salmon to most predators in the system (Willette, 2001; this volume) probably resulted in strong

selection for foraging behaviours that maximized feeding and growth rates.

But foraging in risky offshore habitats would not lead to greater reproductive success unless either the density or type of food available to juveniles limited growth in nearshore habitats. In PWS, growth rates of CWT juvenile salmon were reduced when zooplankton density was low and the number of juveniles in hatchery release groups exceeded 20 million (Fig. 15). Energy content of juvenile salmon was also lower in areas near hatcheries where juvenile salmon densities were high compared with areas distant from hatcheries in eastern PWS (Paul and Willette, 1997). Limitation of feeding rates in nearshore habitats probably extended the salmon's period of vulnerability to predators, increased size-dependent predation losses as foraging juveniles dispersed offshore (Willette, 2001; this volume p. 110), and decreased the probability that salmon would reach the critical size necessary to survive their first winter (Beamish and Mahnken, 1999).

Our numerical model simulations suggested another process that could lead to selection for foraging behaviours that maximized growth rates. When salmon densities are above the satiation threshold, the best survival strategy for salmon should be to minimize their overlap (encounter rate) with predator distributions by schooling or staying in nearshore habitats. However, this strategy can only be successful if salmon maintain high growth rates (Fig. 13). Thus, selection for foraging behaviours that maximize growth would increase the reproductive success of salmon exposed to a satiated predator population.

Our size-refuge hypothesis was supported by analyses of predator stomach contents, estimates of vulnerabilities of salmon to four predator groups, and simulated salmon growth trajectories (Table 2). Predation on juvenile salmon was size dependent, but the nature of the dependency was a function of predator and prey sizes. Relative vulnerabilities of salmon to small planktivores and piscivores decreased over salmon lengths from 3 to 7 cm, but increased over this same length range for large planktivores (Willette, 2001; this volume p. 110). When simulated predation was shifted from May to June, the vulnerability of salmon to predators became more dependent on salmon growth than initial size. But, the size- and growth-dependent vulnerabilities of salmon differed more among predator groups than between May and June suggesting that changes in the composition of predator fields could more strongly affect the nature of size-dependent predation losses of salmon than changes in the timing of predation events.

The sizes at which juveniles reach a refuge from predation depends upon the size composition of the predator

field. Fish typically do not consume prey greater than 50% of their length (Popova, 1978), and capture success rates decline rapidly when preys become a large proportion of predator size (Miller et al., 1988). Our model simulations indicated that adult pollock were an important predator in PWS, and estimates of total consumption of salmon from field studies suggested that small planktivores and piscivores were also important. In a system dominated by adult pollock (given the typical range of growth), juvenile salmon would not likely reach a size refuge from predation during the initial 60 days of sea life. However, in a system dominated by small planktivores and piscivores, salmon entering the ocean at a large size or exhibiting high growth rates would likely reach a size refuge (Willette, 2001; this volume p. 110).

The nature of size-dependent predation losses integrated over the juvenile period is a function of the composition of the predator field and the timing of predation events. Our field data indicated that predation events could be modulated by changes in predator abundance, the abundance of alternative prey (Figs 12 and 14), or juvenile salmon foraging behaviour (Willette, 2001; this volume p. 110), however, our numerical model simulations suggested that the timing of predation events could also be affected by predator size or salmon density. When high-density aggregations of salmon are released, predation events could be shifted later in the juvenile period because salmon densities will tend to remain above the satiation threshold for a longer period of time. In a system dominated by adult pollock, predation events could be shifted earlier in the juvenile period because the satiation threshold for the larger predator occurs at higher salmon densities. When the timing of predation events is shifted later in the juvenile period and small planktivores and piscivores are the dominate predator, juveniles that sustained higher growth rates earlier in the season will tend to suffer lower predation losses (Willette, 2001; this volume). The converse will be true in a system dominated by large planktivores. Predation events occurring early in the juvenile lifestage will not produce this effect, due to lack of sufficient time for growth to alter juvenile sizes. In this case, sizes of juveniles upon ocean entry will determine size-dependent predation losses not growth differences.

Our results indicate that bottom-up processes affecting the duration of the spring bloom, and juvenile salmon growth and foraging behaviour also modify top-down processes involving foraging mode shifts toward piscivory and size-dependent predation losses of juvenile salmon. Physical conditions that maintain a weakly stratified surface layer and prolonged *Neocalanus* bloom (Eslinger et al., 2001; this volume p. 81) will probably accelerate juvenile salmonid growth if food is limiting

and shelter juveniles from predation for a longer time. The converse may be true when the surface layer is more strongly stratified. These interactions between bottom-up and top-down processes result from the dominance of facultative planktivores as salmonid predators and the nature of salmon foraging behaviours.

FUTURE RESEARCH

The current version of our foraging-physiology-dispersion model contains a subset of all of the processes thought to be important in determining the mortality of juvenile pink salmon. Future modelling efforts should incorporate the size composition of the juvenile salmon population and a cross-passage spatial dimension. These modifications to the model will allow us to examine juvenile salmon foraging behaviour and predation risk, as well as density and size effects on juvenile salmon stock interactions. These simulations should also include piscivore predators. Analyses should be conducted to examine the sensitivity of model predictions to various model parameters, and the information obtained from this should be used to focus future monitoring to measure model inputs and validate model predictions.

Our analyses have indicated the importance of multiple CWT groups of salmon released at various sizes, densities, and times during the spring bloom for validating model predictions. Our field and modelling efforts have determined (i) the importance of predator size and salmon densities in determining the nature of mortality processes; (ii) the difficulty of measuring total predation losses of salmon; (iii) the usefulness of numerical models when coupled with multidimensional validation for identifying important predators and understanding mortality processes; and (iv) that patterns of salmon survival by date of release are likely established within PWS. Future field studies should focus on developing methods to measure juvenile salmon densities and partition estimates of salmon survival between juvenile and oceanic lifestages. Continued tagging of multiple groups will be critical to further model validation and ultimately to using models to understand mortality processes.

ACKNOWLEDGEMENTS

must go to those who initiated and constructed the Sound Ecosystem Assessment program. The Prince William Sound Ecosystem Research Planning Group, composed of those having the greatest stake in the success of this endeavour, guided the development and implementation of this research effort. This project was funded in part by the *Exxon Valdez* Oil Spill Trustee Council. However, the findings presented by the authors are their own and do not represent the position of the Trustee Council. The modelling research plan was the result of a 1993 grant from the Institute for Systems Research and from the Advanced Visualization Laboratory, both of the University of Maryland. The development of this synthesis was made possible by support from the Alaska Department of Fish and Game and by the financial support from two sources of private investment in the pink salmon model.

REFERENCES

Armstrong, R.H. and Winslow, P.C. (1968) An incidence of walleye pollock feeding on salmon young. *Trans. Am. Fish Soc.* **97**:202–203.

Bailey, K.M. and Houde, E.D. (1989) Predation on eggs and larvae of marine fishes and the recruitment problem. *Adv. Mar. Biol.* **25**:1–83.

Bakshtanskiy, E.L. (1964) Effect of predators on the young of *Oncorhynchus gorbuscha* and *Oncorhynchus keta* in the White and Barents Seas. *Voprosy Ikhtiologii* **4**:136–141.

Bakshtansky, E.L. (1965) The impact of the environmental factors on survival of the far eastern young salmon during the acclimatization of the latter in the northwest part of the USSR. *ICNAF Environ. Symposium*, Spec. Publishers no. 6, 477–479.

Bax, N.J. (1983) Early marine mortality of marked juvenile chum salmon released into Hood Canal, Puget Sound, Washington, in 1980. *Can. J. Fish. Aquat. Sci.* **40**:426–435.

Beamish, R.J. and Mahnken, C. (1999) Taking the next step in fisheries management. Proceedings of a symposium on ecosystem considerations in fisheries management. Fairbanks: University of Alaska Sea Grant College Program 99–01: 1–22.

Brett, J.R. and Higgs, D.A. (1970) Effect of temperature on rate of gastric evacuation in fingerling sockeye salmon (*Oncorhynchus nerka*). *J. Fish. Res. Board Can.* **27**:1767–1779.

Cooney, R.T. (1986) Zooplankton. In: *The Gulf of Alaska, Physical Environment and Biological Resources.* D.W. Hood and S.T. Zimmerman (eds). Anchorage: U.S. Department of Commerce, Minerals Management Service, 285–304.

Conover, W.J. (1999) Practical nonparametric. *Statistics.* New York: John Wiley & Sons, Inc.

Cooney, R.T., Urquhart, D. and Barnard. D. (1981) The behavior, feeding biology, and growth of hatchery-released pink and chum salmon fry in Prince William Sound, Alaska. Fairbanks: University of Alaska Sea Grant College Program 81–5: p. 114.

Cooney, R.T., Willette, T.M., Sharr, S., Sharp, D. and Olsen, J. (1995) The effect of climate on North Pacific pink salmon (*Oncorhynchus gorbuscha*) production: examining some details of a natural experiment. In: *Climate Change and Northern Fish Populations.* R.J. Beamish (ed.). *Can. Spec. Pub. Fish. Aquat. Sci.* **121**:475–482.

Cooney, R.T., Allen, J.R., Bishop, M.A., Eslinger, D.L., Kline, T., Norcross, B.L., McRoy, C.P., Milton, J., Olsen, J., Patrick, V., Paul, A.J., Salmon, D., Scheel, D., Thomas, G.L., Vaughan, S.L., and Willette, T.M. (2001a) Ecosystem controls of juvenile pink salmon (*Onchorynchus gorbuscha*) and Pacific herring (*Clupea pallasi*) populations in Prince William Sound, Alaska. *Fish. Oceanogr.* **10**(Suppl. 1):1–13.

Cooney, R.T., Coyle, K.O., Stockmar, E. and Staark, C. (2001b) Seasonality in surface-layer net zooplankton communities in Prince William Sound, Alaska. *Fish. Oceanogr.* **10**(Suppl. 1): 97–109.

Coyle, K.O. and Paul, A.J. (1992) Interannual differences in prey taken by capelin, herring, and red salmon relative to zooplankton abundance during the spring bloom in a southeast Alaska embayment. *Fish. Oceanogr.* **1**:294–305.

Cushing, D.H. (1967) The grouping of herring populations. *J. Mar. Biol. Ass., U.K., N.S.* **47**:193–208.

Dwyer, D.A., Bailey, K.M. and Livingston, P.A. (1987) Feeding habits and daily ration of walleye pollock (*Theragra chalcogramma*) in the eastern Bering Sea, with special reference to cannibalism. *Can. J. Fish. Aquat. Sci.* **44**:1972–1984.

Eslinger, D.L., Cooney, R.T., McRoy, C.P., Ward, A., Kline, T., Simpson, E.P., Wang, J. and Allen, R.J. (2001) Plankton dynamics: observed and modelled responses to physical conditions in Prince William Sound, Alaska. *Fish. Oceanogr.* **10**(Suppl. 1):81–96.

Geiger, H.J. (1990) Pilot studies in tagging Prince William Sound pink salmon with coded-wire tags. Alaska Department of Fish and Game. *Fish. Res. Bull.* 90–102.

Godin, J.-G.J. (1981) Daily patterns of feeding behavior, daily rations, and diets of juvenile pink salmon (*Oncorhynchus gorbuscha*) in two marine bays of British Columbia. *Can. J. Fish. Aquat. Sci.* **38**:10–15.

Hartt, A.C. (1980) Juvenile salmonids in the oceanic ecosystem – the critical first summer. In: *Salmonid Ecosystems of the North Pacific*, W.J. McNeil and D.C. Himsworth (eds). Corvallis: Oregon State University Press, 25–57.

Haynes, E., Rutecki, T., Murphy, M. and Urban, D. (1995) Impacts of the *Exxon Valdez* oil spill on bottomfish and shellfish in Prince William Sound. Anchorage: Final report to the Exxon Valdez Oil Spill Trustee Council, fish/shellfish study no. 18.

Healey, M.C. (1982) Timing and relative intensity of size-selective mortality of juvenile chum salmon during early sea life. *Can. J. Fish. Aquat. Sci.* **39**:952–957.

Helfman, G.S. (1993) Fish behaviour by day, night and twilight. In: *Behaviour of Teleost Fishes*, 2nd edn. T. J. Pitcher (ed.). New York: Chapman & Hall, 285–305.

Hepler, K.R., Hansen, P.A. and Bernard, D.R. (1994) Impact of oil spilled from the *Exxon Valdez* on survival and growth of Dolly Varden and cutthroat trout in Prince William Sound, Alaska. Anchorage: Final report to the Exxon Valdez Oil Spill Trustee Council, fish/shellfish study no. 5.

Holling, C.S. (1959) The components of predation as revealed by a study of small mammal predation of the European pine sawfly. *Can. J. Entomol.* **91**:385–398.

Hollowed, A.B., Brown, E., Megrey, B.A. and Wilson, C. (1996) Walleye pollock. In: *Stock Assessment and Fishery Evaluation Report for Groundfish Resources of the Gulf of*

Alaska. Anchorage: North Pacific Fishery Management Council, Gulf of Alaska Groundfish Plan Team.

Ito, S. (1992) Diffusion equations. Translations of mathematical monographs. *Providence: Amer. Math. Soc.* **114**.

Jewett, S.C. and Dean, T.A. (1997) The effects of the *Exxon Valdez* oil spill on eelgrass communities in Prince William Sound, Alaska 1990–95. Anchorage: Final report to the Exxon Valdez Trustee Council, restoration project 95106: p. 92.

Jewett, S.C., Dean, T.A., Smith, R.O., Stekoll, M., Haldorson, L.J., Laur, D.R. and McDonald, L. (1995) The effects of the *Exxon Valdez* oil spill on shallow subtidal communities in Prince William Sound, Alaska, 1989–93. Anchorage: Final Report to the Exxon Valdez Trustee Council, Restoration Project, 93047, p. 75.

Karpenko, V.I. (1998) Ocean mortality of northeast Kamchatka pink salmon and influencing factors. *N. Pac. Anad. Fish Comm. Bull.* **1**:251–261.

Kirsch, J. (1997) Acoustic biomass estimate of adult walleye pollock in Prince William Sound, Alaska, in winter 1997. Cordova: Prince William Sound Science Center. Final report to the Alaska Department of Fish and Game.

MacLennan, D.N. and Simmonds, E.J. (1992) *Fisheries Acoustics.* London: Chapman & Hall.

Miller, T.J., Crowder, L.B., Rice, J.A. and Marschall, E.A. (1988) Larval size and recruitment mechanisms in fishes: toward a conceptual framework. *Can. J. Fish. Aquat. Sci.* **45**:1657–1670.

Morstad, S., Sharp, D., Wilcock, J. and Johnson, J. (1997) Prince William Sound area 1996 annual finfish management. *Report.* Anchorage: Alaska Department of Fish and Game. Regional Information Report no. 2A97–17.

Parker, R.R. (1968) Marine mortality schedules of pink salmon of the Bella Coola River, central British Columbia. *J. Fish. Res. Bd. Can.* **25**:757–794.

Parker, R.R. (1971) Size selective predation among juvenile salmonid fishes in a British Columbia inlet. *J. Fish. Res. Bd. Can.* **28**:1503–1510.

Patrick, V., Mason, D.M., Willette, T.M., Cooney, R.T., Nochetto, R.H., Allen, J.R., Rao, S.P. and Kulkarni, R. (2001) A time evolution representation of the marine subsystem associated with hatchery reared pink salmon fry and the post-release period of outmigration in Prince William Sound, Alaska. Technical Report TR 2001-XX, Institute for Systems Research, University of Maryland.

Paul, A.J. and Willette, T.M. (1997) Geographical variation in somatic energy content of migrating pink salmon fry from Prince William Sound: a tool to measure nutritional status. *Forage fishes in Marine Ecosystems.* Fairbanks: University of Alaska Sea Grant Program Report 97–01: 707–720.

Paul, A.J., Paul, J.M. and Smith, R.L. (1993) The seasonal changes in somatic energy content of Gulf of Alaska yellowfin sole, *Pleuronectes asper. J. Fish Biol.* **43**:131–138.

Paulsson, G.C. (1998) Lingcod and rockfish management: abundance and distribution estimation. Olympia: Final report to Federal Aid in Sport Fish Restoration, Washington Department of Fish & Wildlife, p. 50.

Platt, T., Brawn, V.M. and Irwin, B. (1969) Caloric and carbon equivalents of zooplankton biomass. *J. Fish. Res. Bd. Can.* **20**:2345–2349.

Popova, O.A. (1978) The role of predaceous fish in ecosystems. In: *Ecology of Freshwater Fish Production*, S.D. Gerking (ed.). New York: John Wiley and Sons.

Ricker, W.E. (1976) Review of the growth rate of and mortality of Pacific salmon in salt water, and non-catch mortality caused by fishing. *J. Fish. Res. Bd. Can.* **33**:1483–1524.

Scheel, D. and Hough, K.R. (1997) Salmon fry predation by seabirds near an Alaskan hatchery. *Mar. Ecol. Prog. Series* **156**:35–48.

Sissenwine, M.P. (1984) Why do fish populations vary? In: *Exploitation of Marine Communities*, R.M. May (ed.). New York: Springer-Verlag, 59–94.

Smith, R.L. and Paul, A.J. (1986) A theoretical energy budget for juvenile walleye pollock in Alaskan waters. *Int. N. Pac. Fish. Comm. Bull.* **47**:79–85.

Smith, R.L., Paul, A.J. and Paul, J.M. (1986) Effect of food intake and temperature on growth and conversion efficiency of juvenile walleye pollock (*Theragra chalcogramma*): a laboratory study. *J. Cons. Int. Explor. Mer.* **42**:241–253.

Smith, R.L., Paul, J.M. and Paul, A.J. (1989) Gastric evacuation in walleye pollock (*Theragra chalcogramma*). *Can. J. Fish. Aquat. Sci.* **46**:489–493.

Sogard, S.M. (1997) Size-selective mortality in the juvenile stage of teleost fishes: a review. *Bull. Mar. Sci.* **60**:1129–1157.

Sokal, R.R. and Rohlf, F.J. (2000) Biometry: the principles and practice of statistics in biological. *Research.* New York: W.H. Freeman.

Sturdevant, M.V., Wertherimer, A.C. and Lum, J.L. (1996) Diets of juvenile pink and chum salmon in oiled and non-oiled nearshore habitats in Prince William Sound, 1989–90. *Am. Fish. Soc. Symp* **18**:578–592.

Thomas, G.L., Patrick, E.V., Kirsch, J. and Allen, J.R. (1997) Development of a multi-species model for managing the fisheries resources of Prince William Sound. In: *Developing and Sustaining World Fisheries Resources – the State of Science and Management.* D.A. Hancock, D.C. Smith, A. Grant and J.P. Beumer (eds). Collingwood: CSIRO Publishing, 606–613.

Thomas, G.L., Kirsch, J., Steinhart, G.B. and Peters, N. (1998) Nekton-plankton acoustics. In: *Sound Ecosystem Assessment.* Anchorage: Annual report to the Exxon Valdez Trustee Council, restoration project no. 97320.

Thorne, R.E. (1983) Assessment of population abundance by hydroacoustics. *Biol. Oceanogr.* **2**:254–261.

Thorsteinson, F.V. (1962) Herring predation on pink salmon fry in a southeastern Alaska estuary. *Trans. Am. Fish Soc.* **91**:321–323.

Traynor, J.J. and Ehrenberg, J.E. (1979) Evaluation of the dual-beam acoustic fish target strength method. *J. Fish. Res. Bd. Can.* **36**:1065–1071.

Wertheimer, A.C. and Celewycz, A.G. (1996) Abundance and growth of juvenile pink salmon in oiled and non-oiled locations of western Prince William Sound after the *Exxon Valdez* oil spill. *Am. Fish. Soc. Symp.* **18**:518–532.

West, C.J. and Larkin, P.A. (1987) Evidence of size-selective mortality of juvenile sockeye salmon (*Oncorhynchus nerka*) in Babine Lake, British Columbia. *Can. J. Fish. Aquat. Sci.* **44**:712–721.

Willette, T.M. (1996) Impacts of the *Exxon Valdez* oil spill on the migration, growth, and survival of juvenile pink salmon in Prince William Sound. *Am. Fish. Soc. Symp.* **18**:533–550.

Willette, T.M. (2001) Foraging behaviour of juvenile pink salmon (*Oncorhynchus gorbuscha*) and size-dependent predation risk. *Fish. Oceanogr.* **10**(Suppl. 1):110–131.

Willette, T.M., Carpenter, G. and Debevec, E. (1995a) Salmon growth and mortality. In: *Sound Ecosystem Assessment*. Anchorage: Annual report to the Exxon Valdez Trustee Council, restoration project no. 94320.

Willette, T.M., Debevec, E. and Johnson, J. (1995b) Salmon predation. In: *Sound Ecosystem Assessment*. Anchorage: Annual report to the Exxon Valdez Trustee Council, restoration project no. 94320.

Willette, T.M., Sturdevant, M. and Jewett, S. (1997) Prey resource partitioning among several species of forage fishes in Prince William Sound, Alaska. *Forage fishes in Marine Ecosystems*. Fairbanks: University of Alaska Sea Grant Program Report 97–01: 11–30.

Willette, T.M., Cooney, R.T. and Hyer, K. (1999a) Predator foraging mode shifts affecting mortality of juvenile fishes during the subarctic spring bloom. *Can. J. Fish. Aquat. Sci.* 56:364–376.

Willette, T.M., Cooney, R.T. and Hyer, K. (1999b) Some processes affecting mortality of juvenile fish during the spring bloom in Prince William Sound, Alaska. *Proceedings of a symposium on ecosystem considerations in fisheries management*. Fairbanks: University of Alaska Sea Grant College Program 99–01: 137–142.

Yoshida, H. (1994) Food and feeding habits of pelagic walleye pollock in the central Bering Sea in summer, 1976–80. Sci. Rep. Hokkaido Fish. Exp. Stn. 45:1–35.